

Consequences of Persistent Mitochondrial DNA Damage and Increased Oxidative Stress

By

Lauren Donoghue

Undergraduate Honors Thesis submitted to the faculty of the Department of Environmental Sciences and Engineering in the Gillings School of Global Public Health at the University of North Carolina at Chapel Hill

Chapel Hill

2014

Approved by:



Advisor: Dr. Leena A. Nylander-French

Advisor: Dr. Joel N. Meyer (Duke University)

Reader: Elena A. Turner (Duke University)

Acknowledgements

Dr. Joel Meyer, the Meyer laboratory group, and Dr. Leena Nylander-French provided the strong support system and encouragement that made this project possible. Dr. Meyer's willingness for me to pursue an honors thesis project in his laboratory and open door not only provided me with a learning-intensive experience that has prepared me for the future, but also instilled the experience-based belief that research is most productive and rewarding when done with great people. The entire Meyer laboratory group contributed to the stimulating environment that made this project a pleasure. Elena Turner provided beneficial mentor support in the laboratory and always helped me think of our research in the context of the bigger picture of toxicology. Ian Ryde dedicated many hours helping me learn how to carry out the experiments successfully and analyze the data, in addition to helping me strengthen my technical skills in the laboratory. Claudia Gonzalez helped significantly with her instruction on statistical analysis/interpretation and in experiments.

Dr. Nylander-French's continued support throughout my time as an undergrad encouraged me to enter the field of toxicology and exposure research with intention, confidence, and high standards for myself. Her encouragement and advice helped me write a thesis I am proud to share. Dr. Jayne Boyer's mentoring and friendship also shaped my laboratory abilities and helped me receive more opportunities for learning.

This work has been supported by the NIH (R01- ES017540-01A2), Duke University Superfund Research Center (Training Core): P42 ES010356, and the UNC Koch Travel Award for presentation at the 2014 Society of Toxicology Annual Meeting.

TABLE OF CONTENTS

ABSTRACT.....	5
List of Figures.....	6
Abbreviations.....	7
1. INTRODUCTION.....	8-13
1.1 Project Background.....	8-11
1.2 Project Aims and Supporting Evidence.....	11-13
2. MATERIALS AND METHODS	
2.1 Nematode Culture.....	14
2.2 UVC Exposures.....	14-15
2.3 Larval Arrest Screening.....	15
2.4 Growth Assay.....	16
2.5 Mitochondrial and Nuclear Genome Copy Number.....	16-17
2.6 Heat Shock Protein Gene Expression.....	18-21
2.7 DNA Damage Assay.....	21-22
2.8 Statistical Analysis.....	22
3. RESULTS	
3.1 Larval Arrest Screening	23-24
3.2 Growth Assay.....	25-31
3.3 Mitochondrial and Nuclear Genome Copy Number.....	31-34
3.4 Heat Shock Protein Gene Expression.....	34-39
3.5 DNA Damage.....	40

4. DISCUSSION

4.1 Larval Arrest Screening	41-42
4.2 Growth Assay.....	42-43
4.3 Mitochondrial and Nuclear Genome Copy Number.....	43-45
4.4 Heat Shock Protein Gene Expression.....	46-49
4.5 DNA Damage.....	50-51
4.6 Future Directions.....	51-52
5. CONCLUSION.....	53
REFERENCES.....	54-57

ABSTRACT

Environmental toxicants such as polycyclic aromatic hydrocarbons can cause irreparable mitochondrial DNA damage. Mitochondria play a critical role in energy production and aging. Mitochondrial dysfunction has been associated with diseases occurring in 1 in 4,000 individuals. In *C. elegans* nematodes, persistent mitochondrial DNA damage during development from exposure to ultraviolet C (UVC) irradiation results in delays in development, reduced ATP production and reduced oxygen consumption and, thus, suggesting dysfunction of the electron transport chain (ETC). The mechanism by which UVC irradiation causes these effects is unclear; one hypothesis is that UVC irradiation-induced mitochondrial dysfunction results in production of reactive oxygen species (ROS). Both ETC dysfunction and UVC exposure can increase levels of ROS associated with increased cellular damage and homeostatic cell signaling. I investigated the larval arrest, growth, genome copy number, and regulation of unfolded protein responses by heat shock proteins in superoxide dismutase (SOD) mutant *C. elegans* with persistent mitochondrial DNA damage to investigate the potential role of increased oxidative stress. Development delay, growth inhibition, and a decrease in mitochondrial-to-nuclear genome copy number, were seen in UVC-exposed mitochondrial SOD mutants compared to UVC-exposed wild-type while cytosolic SOD mutants exhibited altered phenotypes similar to wild-type. No nematode strains showed significant upregulation of mitochondrial, endoplasmic reticulum, or cytosolic heat shock proteins. These results suggest that UVC exposure specifically affects mitochondria and that the effects of the mitochondrial DNA damage are exacerbated by decreased defense against damage caused by mitochondrial superoxide. Further experiments are

needed to determine the mechanism(s) that contribute to these altered phenotypes and the extent of ETC dysfunction due to persistent mitochondrial DNA damage caused by UVC irradiation.

List of Figures

Figure 1. Developmental progression of *C. elegans*

Figure 2. Schematic of UVC exposure protocol (adapted from Leung *et al.*, 2013)

Figure 3. Example of microscopy for Growth Assay

Figure 4. Growth of N2

Figure 5. Growth of *sod-2*

Figure 6. Growth of *sod-3*

Figure 7. Percent unexposed control growth of N2, *sod-2*, *sod-3*

Figure 8. Growth of N2

Figure 9. Growth of *sod-2/3*

Figure 10. Growth of *sod-1/4/5*

Figure 11. Percent unexposed control growth of N2, *sod-2/3*, *sod-1/4/5*

Figure 12. Mitochondrial copy number in N2, *sod-2/3*, *sod-1/4/5*

Figure 13. Nuclear copy number in N2, *sod-2/3*, *sod-1/4/5*

Figure 14. Mitochondrial/nuclear copy number in N2, *sod-2/3*, *sod-1/4/5*

Figure 15. Gene expression of *hsp-6*

Figure 16. Gene expression of *hsp-60a*

Figure 17. Gene expression of *hsp-60b*

Figure 18. Gene expression of *hsp-4*

Figure 19. Gene expression of *hsp-16.2*

Figure 20. Gene expression of *hsp-16.41*

Abbreviations

PAH – polycyclic aromatic hydrocarbon

UVC – ultraviolet C radiation

mtDNA – mitochondrial DNA/genome

ETC – Electron transport chain

OXPPOS – oxidative phosphorylation

ROS – reactive oxygen species

nDNA – nuclear DNA/genome

SOD – superoxide dismutase

MnSOD – manganese-binding superoxide dismutase

Cu/ZnSOD – copper or zinc-binding superoxide dismutase

hsp – heat shock protein

L1, L2, L3, L4 – first, second, third, fourth larval stage of *C. elegans*

N2 – wild-type *C. elegans* strain

ER – endoplasmic reticulum

(UPR^{mt}) – mitochondrial unfolded protein response

(UPR^{ER}) – endoplasmic reticulum unfolded protein response

(UPR^{CYT}) – cytosolic unfolded protein response

PCR – polymerase chain reaction

Ct – cycle threshold values

ANOVA – analysis of variance

1. INTRODUCTION

1.1 Project Background

Mitochondria are fundamental to the health of organisms relying on aerobic cellular respiration for energy. Mitochondrial dysfunction is responsible for a wide variety of mitochondrial diseases that affect about 1 in 4,000 individuals and include diseases that can affect function of vital organs such as the brain, heart, and liver apparently due to their high energy requirements (1,2). Some environmental toxicants and pharmaceuticals such as chemotherapeutics and antiviral drugs have been shown to selectively target mitochondria (3). Exposure to polycyclic aromatic hydrocarbons (PAHs), a group of environmental toxicants found in cigarette smoke and fuel burning byproducts, can irreparably damage mitochondrial DNA (4,5). Unlike the nuclear genome, the mitochondrial genome does not have nucleotide excision DNA repair machinery, which can remove bulky DNA adducts caused by PAH exposure plus other photodimers such as the pyrimidine dimers caused by ultraviolet-C (UVC) irradiation. While there is evidence in both human fibroblasts and *Caenorhabditis elegans* (*C. elegans*) nematodes that mitochondrial DNA (mtDNA) damage is removed through autophagy (6,7) and that over time the DNA damage will be diluted by an increase in mitochondrial genome copy number (7), the mechanisms responsible for removing such mtDNA damage are not fully understood.

The mitochondrial genome is significantly smaller than the nuclear genome in *C. elegans*, with only 13,794 base pairs compared to 100,278,046 base pairs in the nuclear genome (8). The 36 genes in the *C. elegans* mitochondria genome encode proteins of the electron transport chain mechanism (ETC) responsible for the oxidative phosphorylation (OXPHOS) metabolic pathway

and the tRNA and rRNAs required for mitochondrial protein translation (9). OXPHOS is necessary for the production of ATP used as cellular energy.

Exposure to UVC during *C. elegans* development results in pyrimidine dimers that are irreparable in mitochondrial DNA but repairable in nuclear DNA (7). Persistent mitochondrial DNA damage results in larval developmental arrests. In *C. elegans*, development occurs as a progression through four larval stages referred to as L1, L2, L3, and L4 until they reach adulthood and reproductive maturity (as shown in Figure 1). The progression from the L3 (third) to L4 (fourth) larval stage requires OXPHOS. Transition from L3 to L4 is delayed after UVC exposure, suggesting ETC dysfunction (6, 7). Additionally, altered phenotypes observed after exposure to UVC are decreased ATP production, decreased oxygen consumption, and a decreased ratio of mitochondrial-to-nuclear genome copy number that provides additional evidence of possible ETC dysfunction (7).

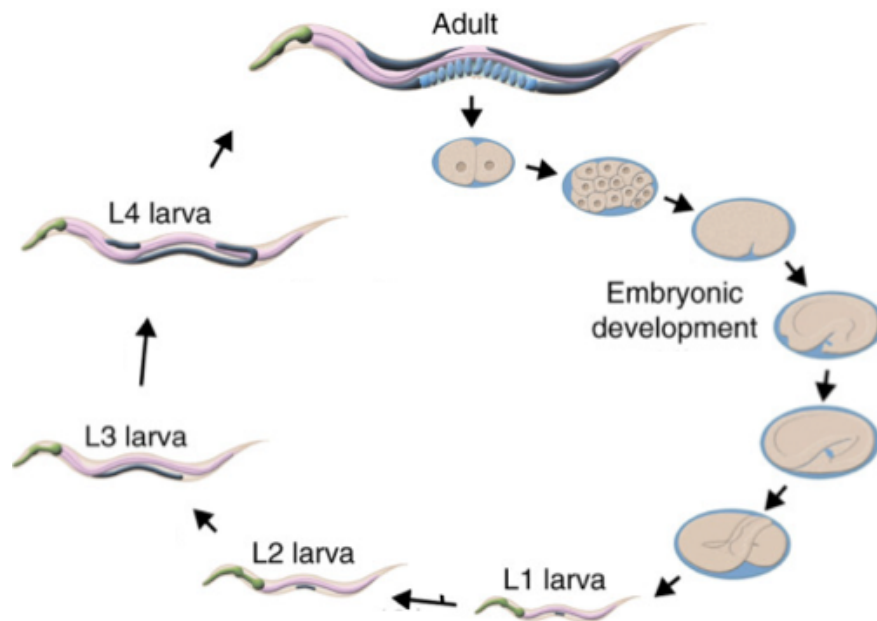


Figure 1. Developmental progression in *C. elegans* (10).

As in humans, the ETC in *C. elegans* consists of five protein complexes encoded by both the nuclear and mitochondrial genomes. These proteins form the ETC from a stoichiometric balance between transcripts from both genomes. The mechanism(s) responsible for ETC dysfunction after persistent mtDNA damage are not currently known. It is postulated that the contributing mechanisms include altered transcription caused by mtDNA damage, increased oxidative damage from reactive oxygen species (ROS), altered cell signaling, an imbalance between the nuclear and mitochondrial proteins of the ETC, and epigenetic modifications.

In this project, I investigated the role of ROS in the ROS-related biological processes of *C. elegans* after exposure to UVC. ROS is a term used for highly reactive oxygen species including hydrogen peroxide, peroxide, hydroxyl ions, and superoxide anions. ROS species have beneficial roles in cells through their participation in cellular signaling and harmful roles in cells through their ability to cause oxidative damage to proteins, DNA, and lipids (11, 12).

Mitochondria are endogenous sources of ROS; for example, under normal function, the ETC reduces 1-2% of the oxygen it uses to superoxide anions (O^{\ominus}) (11, 13). The superoxide anions are primarily a byproduct from the conversion of O_2 to H_2O from the fourth ETC complex, cytochrome C oxidase. Irregular activity of the ETC caused by slower flow of electrons through the chain, the reversed flow of electrons, or an uncoupling of regulation of the electron gradient used by the ETC, can result in an increased production of superoxide anion by the first and third complexes (13-17). The superoxide anions remain in the mitochondria and are not believed to diffuse through the membrane into the cytosol because of their charge and highly reactive nature (11).

Cells have antioxidant enzymes to help prevent the damaging effects of ROS by converting them into less reactive molecules, a process referred to as scavenging. These include

superoxide dismutase (SOD) which converts O^{\ominus} to H_2O_2 , catalase which converts H_2O_2 to H_2O and O_2 , and glutathione peroxidases which converts organic peroxidases to alcohols and H_2O_2 to H_2O (11). Humans have genes encoding three different location-specific SOD enzymes while *C. elegans* have five. These include *sod-2* and *sod-3* which encode mitochondrial SODs that bind manganese (MnSOD), *sod-1* and *sod-5* that encode cytosolic SODs which bind copper and zinc (Cu/ZnSOD), and *sod-4* that encode extracellular SOD and also binds copper and zinc (Cu/ZnSOD). These enzymes convert O^{\ominus} and H^+ into H_2O_2 , H_2O , and O_2 .

The nuclear and mitochondrial genomes of *C. elegans* are mapped, which allows for the use of gene knockout mutants and transgenic strains for the study of their biological processes, many of which are conserved with higher eukaryotes (18). To selectively investigate how persistent mtDNA damage induced by UVC exposure could lead to increased superoxide anion production and oxidative stress from ETC dysfunction, I used several strains of gene knockout *sod* mutants. While SOD deficiencies do not necessarily result in increased oxidative stress, studies have shown that *sod* mutants such as *sod-2* have increased steady-state ROS and superoxide levels (19, 20). In this project, levels of ROS in these mutants are not directly measured, so it can only be assumed and not concluded that superoxide levels are increased. The mutants are understood to have decreased defenses to superoxide anion reactivity. The mutants are used as a genetic approach to indirectly study the effects of environmental exposure to mitochondrial toxicants. Due to their altered genetic makeup, measurement of the effects seen in mutants are considered more conservative than what would occur from environmental exposures to a normal background.

1.2 Project Aims and Supporting Evidence

In a preliminary experiment for this project, *C. elegans* mutants deficient in MnSODs (*sod-2* and *sod-3* single-gene mutants) exposed to UVC had a longer developmental arrest from the OXPHOS-requiring L3 to L4 transition compared to wild-type. This indicated that increased sensitivity to mitochondrial ROS (due to MnSOD deficiency) further inhibited the OXPHOS capacity of nematodes with persistent mtDNA damage.

To further investigate the biological processes underlying these observations, I investigated developmental arrest, growth inhibition, mitochondrial-to-nuclear genome ratio recovery, regulation of heat shock protein genes, and mitochondrial and DNA damage recovery of *sod-2/3* and *sod-1/4/5* mutants, and wild-type (N2) nematodes after exposure to UVC to test hypotheses. The *sod-2/3* double-gene mutants were used to specifically explore the biological processes in the mitochondria that result from decreased defense to superoxide from the ETC. A *sod-1/4/5* triple-gene mutants were used to explore ROS-related biological processes outside of the mitochondria and also served as a unexposed control to the mitochondrial-specific mutants. Additionally, exposure to UVC results in a low level of ROS production. In this project, UVC exposure induced the persistent mtDNA damage studied. Use of the *sod-1/4/5* mutants also allowed for investigation of ROS sensitivity outside of the mitochondria that would likely result from the UVC exposure protocol rather than ETC dysfunction, although superoxide anion is not reported as a primary ROS from UVC exposure (21). Explanation of interest in the specific biological outcomes listed, hypotheses, and evidence of these hypotheses are presented below.

Bess *et al.* (2012) showed a delay in developmental progression or larval arrest from the L3 to L4 stage in N2 *C. elegans* after three exposures to 7.5 J/m² UVC (1). I hypothesized that MnSOD mutants would have a more severe developmental delay as a result of increased oxidative damage to ETC genes or proteins due to their inability to scavenge mitochondrial

superoxide. I also hypothesized that the non-mitochondrial *sod-1/4/5* mutants would have a developmental progression similar to wild-type *C. elegans* because cytosolic or extracellular superoxides are not expected to be involved in the same mechanism of development arrest. In addition, I hypothesized that MnSOD mutants would have inhibited growth during development due to a decreased ability to produce energy for cells while *sod-1/4/5* mutants would have a normal growth.

Leung *et al.* (2013) showed a decrease in mitochondrial-to-nuclear genome copy number ratio throughout the development after exposure to UVC (7). I hypothesized that *sod-2/3* mutants would exhibit a decreased, or comparative to wild-type, mitochondrial copy number due to increased mtDNA damage from ROS in the mitochondria. I also hypothesized that *sod-1/4/5* mutants would exhibit a decreased, or comparative to wild-type, nuclear genome copy number due to increased nuclear DNA (nDNA) damage from cytosolic ROS.

Heat shock proteins (hsp) are molecular chaperone proteins that are upregulated in response to stress (such as oxidative stress) and aid in the proper folding of proteins or degradation of lingering proteins through their role in the unfolded protein responses (22). I hypothesized that N2, *sod-2/3*, and *sod-1/4/5* would all exhibit upregulation of *hsp* genes encoding mitochondrial-localized hsp (hsp-6 and hsp-60) due to the mtDNA damage from UVC exposure. I also hypothesized that *sod-2/3* would exhibit the highest upregulation due to the decreased defenses against mitochondrial ROS. Further, I hypothesized that none of the strains would exhibit upregulation of endoplasmic reticulum hsp (hsp-4), but that all strains would exhibit upregulation of the cytosolic hsp (hsp-16.2 and hsp-16.41), with *sod-1/4/5* showing the greater upregulation due to the decreased defenses against cytosolic ROS.

Bess *et al.* (2012) showed an increase in mtDNA lesions after a single UVC exposure in wild-type nematodes (1). Therefore, the *sod-2/3* mutants were expected to show a slight increase in mtDNA lesions due to increased oxidative mtDNA damage. The *sod-1/4/5* mutants were expected to show a slight increase in nDNA lesions due to increased oxidative nDNA damage.

2. MATERIALS AND METHODS

2.1 Nematode Cultures

All nematode strains were grown and stored at 20°C on K-agar plates seeded with *Escherichia coli* strain OP50. Wild-type N2 (Bristol), *sod-2* (gk257) I, and *sod-3* (tm760) II nematodes were obtained from the *Caenorhabditis* Genetics Center (CGC; Minneapolis, MN, USA). The *sod-2/3* [*sod-2* (gk257) I; *sod-3* (tm760) X] double-mutant strain and *sod-1/4/5* triple-mutant strain [*sod-1* (tm776); *sod-5* (tm1146) II; *sod-4* (gk101) III] were obtained from Bart Braeckman (Ghent University, Ghent, Belgium). Nematode eggs were collected from plates by dissolving gravid adults with a 5% sodium hypochlorite solution. Eggs were hatched in K-medium with MgSO₄, CaSO₄, and cholesterol to obtain developmentally synchronized L1 larvae.

2.2 UVC Exposure

Synchronized L1 nematodes were plated onto unseeded, non-peptone K-agar plates to prevent bacterial growth. This starvation developmentally arrested the nematodes at the L1 stage. For each plate of UVC-exposed nematodes, a plate of unexposed nematodes was maintained under the same conditions in order to provide unexposed controls. After hatching and plating, nematodes were exposed to 7.5 J/m² UVC irradiation three times at 0, 24, and 48 h, as previously described in Bess *et al.* (2012). The exposure time was calculated using a UVX Digital Radiometer (UVP, Inc., Upland, CA) and the equation [time of exposure (sec) = 7.5 J/m² ÷ meter reading (J/m²) / 100] to quantify the radiation (J/m²) emitted from the UVC bulb to

increase consistency between experiments. Exposed and unexposed control nematodes were transferred to OP50-seeded plates after they received the third UVC exposure.

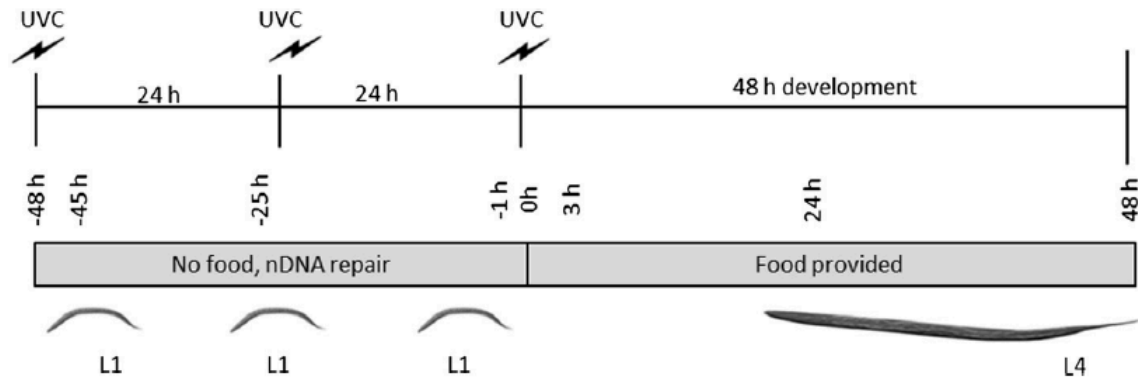


Figure 2. Schematic of UVC exposure protocol (adapted from Leung *et al.*, 2013).

2.3 Larval Arrest Screening

Immediately after the third UVC exposure, individual worms were transferred to individual wells in a 24-well plate. A total six worms were transferred from each UVC-exposed and unexposed control plate. The remaining nematodes were transferred to OP50 seeded plates for growth measurements. Wells were filled with K-agar and seeded with OP50. At 24, 48, 72, and 96 h after the last UVC exposure, the developmental stage of each nematode was recorded according to the developmental stages described in Figure 1. The L4 stage is uniquely identified by a vulva “crescent” that appears on the side of hermaphrodite nematodes. Before observations were recorded, plate labels were covered and plates were randomized to reduce potential recording bias. The developmental stage of the nematodes was also observed at each time point on OP50 plates for growth measurements as unexposed controls to ensure that the conditions in the 24-well plates were not affecting development. This experiment was repeated three times (a total sample size of $n = 18$).

2.4 Growth Assay

At 24, 48, 72, and 96 h after the last UVC exposure, 100-200 nematodes were rinsed from plates with K-medium and collected in 2-mL microcentrifuge tubes. Tubes were stored at -20°C for at least 20 min to kill the nematodes. Tube labels were covered with a randomized number to reduce potential bias when measuring samples. Nematode pellet (10 µL) was placed on a thin K-agar pad on a glass slide. Using an Axioskop fluorescent microscope (Zeiss, Germany) and 10X objective, 15 or 20 nematodes on each slide were measured by tracing the outer body-line from the tip of the tail to the middle of the mouth using NIS Elements Basic Research software (v. 3.2, Nikon Instruments, Inc., Melville, NY). Each plate was observed for gravid adults and egg hatching at each time point to recognize progeny that was present on slide samples. Averages and standard deviations were calculated for each set of 20 measurements/sample. Statistical analyses were carried out as described in section 2.8.

2.5 Mitochondrial and Nuclear Genome Copy Number

2.5.1 Sample Collection

Six nematodes were picked into 90 µL of 3X lysis buffer (25 mM tricene, 80 mM potassium acetate, 10% (w/v) glycol, 2.25% (v/v) DMSO, and Sigma H₂O) at 24, 48, and 72 h after the last UVC exposure in triplicate. Samples were frozen on dry ice and stored at -80°C until analysis. To lyse nematode samples, samples were taken directly from -80°C and placed in a thermal cycler (Biometra T1) for 60 min at 65°C followed by 15 min at 95°C.

2.5.2 Real-time PCR

Reactions were carried out largely as described previously by Leung *et al.* (2013) (7). Primers for the nuclear gene *cox-4* were used to measure nuclear copy number and primers for the mitochondrial gene *nd-1* were used to measure mitochondrial DNA copy number. Real-time PCR reactions contained 2 μL of lysed sample, 12.5 μL of SYBR Green PCR Master Mix (Applied Biosystems), 2.0 μL of forward and reverse primers at 5 μM (400 μM final concentration) and 8.5 μL H_2O . Samples were run in triplicate. Reactions were amplified in the 7300 Real Time PCR System (Applied Biosystems) for 2 min at 50°C, 10 min at 95°C, 40 cycles of 15 sec at 95°C, and then 60 sec at 60°C. Dissociation temperature curves were generated and assessed for each sample to ensure a singular product.

A sample of sterilized 20 *glp-1* nematodes in 20 μL were diluted to make a standard curve of 1568, 784, 392, 196, 98, and 49 nuclear genome copies and run as described above. A plasmid with a mitochondrial genome insert was diluted and used to prepare a standard curve of 64,000, 48,000, 32,000, 24,000, 16,000, 12,000, 8,000, 6,000, and 4,000 mitochondrial genome copies (23).

The real-time PCR cycle threshold (Ct) values were averaged across biological triplicates. Copy number values were then calculated using the equation of a logarithmic curve created from the standard values for the PCR reactions. These output values were averaged as the biological triplicates across experiments. Statistical analyses were carried out as described in section 2.8.

2.6 Heat Shock Proteins - Gene Expression Measurements

2.6.1 Real-time PCR Primers and Optimization

Sequences of the *C. elegans* heat shock protein genes were obtained online from <http://www.wormbase.org/>. Two isoforms of the *hsp-60* gene were noted. The modified sequences were inputted to the Primer 3 online software for primer design (<http://bioinfo.ut.ee/primer3/>). Default settings were accepted after modifying the desired product length to be 75 – 200 base-pairs. Output-primer sequences were considered if the annealing temperatures were less than 1.5 degrees between the forward and reverse primers, GC content was near 50%, and the primers covered the intron/exon junctions. Three test primers were ordered for each gene (Integrated DNA Technologies, Coralville, IA).

All test primers were used in the real-time PCR reactions with reverse transcribed existing N2 RNA. All primers were run in reactions with annealing/extension temperatures of 56°C, 58°C, 60°C, and 62°C to find optimal temperatures (allowed for Ct values between 19-22) and primers that created single products (dissociation stages and analysis were added). Product sizes were analyzed by gel electrophoresis. Two percent agar gels were produced with agar, 50 µL SB buffer (1x), and 5 µL Syber Safe (Invitrogen, Carlsbad, CA). A 5-µl sample of Hyper ladder V was used as a ladder (Invitrogen). Cyan yellow buffer (6x) was mixed with each sample at 1.25 µL cyan yellow buffer and 9 µL sample for a total of 10.15 µL in 10 µL wells. Product sizes were checked against the projected product lengths for the test primers and confirmed.

Sequences of the best primer-pairs for each gene were as follows:

hsp-4: Forward: CGTTCAAGATCGTCGACAAGT

Reverse: GACCAAGGTAGGATTCGGCA

Product size: 138 base pairs

hsp-6: Forward: TCGTGTCATCAACGAGCCAA
Reverse: AGCGATGATCTTATCTCCAGCG

Product size: 76 base pairs

hsp-16.2: Forward: CGCCAAAGAAAGAAGCGGTT
Reverse: CTTCGACGATTGCCTGTTGA

Product size: 60 base pairs

*This primer does not overlap an exon-exon junction

hsp-16.41: Forward: TGGACGAACTCACTGGATCTG
Reverse: TGAGAGACATCGAGTTGAACCG

Product size: 133 base pairs

hsp-60a: Forward: AGGCTCTTACCACTCTTGTTCT
Reverse: CTCCCGTCGCAATTCCCATA

Product size: 123 base pairs

hsp-60b: Forward: CCAAGAAGGTCACCATCACC
Reverse: TCTGTTTGATCTCCACGCCC

Product size: 64 base pairs

2.6.3 Nematode Sample Collection

At 24, 48, and 72 h after the last UVC exposure, ~20,000 nematodes were rinsed with K-medium from plates into 15-mL tubes. Samples were placed on a shaker for 10 min at 20°C to allow for OP50 purging. Samples were centrifuged at 2200 rpm for 2 min. Pellets were then transferred to 2-mL microcentrifuge tubes and centrifuged at 2000 rpm for 1 min. K-medium was vacuumed from the tubes and replaced with 1 mL of RLT buffer (RNeasy Mini Kit; Qiagen, Valencia, CA)

and 0.1 mL of beta-mercaptoethanol. Samples were immediately frozen in liquid nitrogen and stored at -80°C until analysis. There were six biological replicates for 24 and 48 h, and four biological replicates at 72 h.

2.6.4 mRNA Extraction

Samples were thawed at 37°C and transferred to 1.7-mL microcentrifuge tubes filled with 0.5 mL of zirconia/silica beads (Next Advance, Inc, Averill Park, NY) Tube caps were double wrapped with Parafilm to prevent leaking during beadbeating. Samples were then placed into Bullet Blender (Next Advance, Inc, Averill Park, NY) and beaten for 30 sec at the speed of 10 followed by transfer to ice to cool for 1 min. This process was repeated for an average of 15 repetitions and samples were checked after 7th, 10th, and 15th repetition to ensure homogeneous lysis. Parafilm was replaced as needed. RNA was then extracted from lysed samples according to the instructions provided with RNeasy Mini Kit (Qiagen). RNA quantity and quality was assessed with spectrometry (NanoDrop 8000 spectrophotometer; Thermo Scientific, Waltham, MA) RNA quality was assessed based on the reported 260/280 values (2.0 optimal for RNA) and 260/230 values (2.0-2.2 optimal for RNA).

2.6.5 Reverse-transcription

The reverse-transcription reactions were carried out using the High Capacity cDNA Reverse Transcription Kit (Applied Biosystems, Grand Island, NY) according the manufacturers instructions. Reactions used 75, 120, or 500 ng of isolated RNA depending on the total quantity isolated for each sample. The reaction was carried out in a thermal cycler (Biometra T1, Goettingen, Germany) for 10 min at 25°C followed by 2 h at 37°C.

2.6.6 Real-time PCR

Real-time PCR reactions contained 2 μL of cDNA diluted to 2 ng/ μL from the reverse-transcription reactions, 12.5 μL of SYBR Green PCR Master Mix (Applied Biosystems), 2.0 μL primers at 5 μM (400 μM final concentration), and 8.5 μL H_2O in optical 96-well plates (MicoAmp Optical, Applied Biosystems). Samples were run in triplicate. Reactions were amplified in the 7300 Real-Time PCR System (Applied Biosystems) for 2 min at 50°C, 10 min at 95°C, 40 cycles of 15 sec at 95°C, and then 60 sec at 56°C. Dissociation temperature curves were generated and assessed for each sample to ensure a singular product. Reactions were also run for housekeeping genes *cdc-42* and *pmp-3*.

The Ct values for each gene were averaged by the sets of biological triplicates or duplicates. These averages were converted to the fold-change of amplification compared to the Ct values of each housekeeping gene. Average fold-changes were averaged across experimental triplicates. The final average taken was the average of the fold-change respective to each housekeeping gene. Statistical analyses were carried out as described in section 2.8.

2.7 DNA Damage Assay

2.7.1 Sample Collection

The same lysate samples used for copy number measurements (see section 2.5) were used for the DNA damage measurements.

2.7.2 Long-amplicon Quantitative PCR and PicoGreen dsDNA Quantification

Reactions were carried out largely as described by Santos *et al.* (2006), with the only modification being the use of Long Amp Hot Start Taq 2X Master Mix (New England BioLabs,

Ipswich, MA) according to the manufacture's instructions for PCR amplification. The PCR protocol was cycle optimized by running template dilutions at 50%, 25%, and 12.5% to determine at which cycle the PicoGreen fluorescence readings matched these dilutions for each strain and time point.

2.7.3. *Data analysis*

Analyses were carried out as described by Santos et al. (2006). DNA lesions are reported as lesion per kilo-base of DNA. These values are scaled to copy number.

2.8 Statistical analysis

Three-factor and two-factor analysis of variance (ANOVA) statistical analyses were carried out using JMP Pro (v. 11: SAS Institute Inc., Cary, NC) to indicate significant effects of strain and/or exposure and/or time at α -level 0.05. Degrees of freedom used were calculated as the product of one less than each of the levels of factors considered or compared. Strain had up to three levels (N2, *sod-2*, *sod-3* or N2, *sod-2/3*, *sod-1/4/5*), exposure had two levels (unexposed control or exposed), and time had up to four levels (24, 48, 72, and/or 96 h). An interaction between factors is described when statistical analysis indicates one factor altering how another factor affects the outcome. When strain, exposure, and time factors had significance together in a three-factor ANOVA, it was considered as a global ANOVA significance. Tukey's Honest Significant Difference (HSD) test was used for post-hoc analyses at α -level of 0.05 in cases of a statistically significant interaction between factors (also in JMP Pro).

3. RESULTS

3.1 Larval Arrest Screening

Variation within strain and treatment development was apparent during observations. The most frequently observed development stage is reported and the second most observed stage is listed in parenthesis to provide understanding of the direction of variation (Table 1 and Table 2).

Variation in growth was largest in UVC-exposed mutants, with up to ~40% of nematodes differing in either direction from the stage listed first.

Table 1. Average larval development stages for N2, *sod-2*, and *sod-3* (n = 24) at 24, 48, 72, or 96 h after the last UVC exposure.

Time (h)	N2 unexposed control	N2 UVC	<i>sod-2</i> unexposed control	<i>sod-2</i> UVC	<i>sod-3</i> unexposed control	<i>sod-3</i> UVC
24	L3	L3	L3 (L2)	L2	L3 (L2)	L2
48	L3 (early L4)	L3	L3 (early L4)	L2 (early L3)	L3 (early L4)	L3 (L2)
72	Gravid adults	Young adult	Adult	L3	Gravid adults	L3 (L4)
96	Adults with L1 progeny	Adult	Adults with L1 progeny	L3	Adults with L1 progeny	Gravid adults

Table 2. Average larval developmental stages N2, *sod-2/3*, and *sod-1/4/5* (n = 24) at 24, 48, 72, or 96 h after the last UVC exposure

Time (h)	N2 unexposed control	N2 UVC	<i>sod-2/3</i> unexposed control	<i>sod-2/3</i> UVC	<i>sod-1/4/5</i> unexposed control	<i>sod-1/4/5</i> UVC
24	L3	L3 (L2)	L3	L3 (L2)	L3	L3 (L2)
48	L4 (young adult)	L3 (late L4)	L3 (early L4)	L3 (L4)	L4 (young adult)	L3
72	Gravid adults	Adult	Young adults	L3 (L4)	Gravid adults	Young adults
96	Adults with L1 progeny	Gravid adults	Adults with L1 progeny	Young adults (gravid adults)	Adults with L1 progeny	Gravid adults

Wild-type larvae maintained at 20°C and not starved on non-peptone plates would be expected to reach the L4 stage at ~24 h, mature adulthood at ~48 h, and be gravid/lay eggs at ~72 h. In Table 1 and Table 2, the developmental progression of N2 unexposed controls after starvation shows that overall development progresses more slowly during the first 48 h due to the period of starvation required for the UVC exposure protocol but then progresses naturally without arrest at any stage and reach maturity at 72 h as expected. The results indicate that strain unexposed control groups had slight differences in development, such as between N2 control at 72 h compared to *sod-2/3* control at 72 h as presented in Table 2. These differences are not surprising as mutants can sometimes develop or growth slightly differently at baseline because of possibly altered steady state conditions. This difference was seen in the *sod-2/3* unexposed controls compared to N2 as a slightly slower development progression at 48 and 72 h. This difference was not seen in the *sod-1/4/5* mutants. It was not recorded for the *sod-2* or *sod-3* mutants, although it is predicted there may have been a slight difference that was not recorded based on the *sod-2/3* results. The developmental stage scoring results presented in Table 1 show a temporary and short larval arrest from the L3 to L4 stage transition in N2 UVC-exposed nematodes from 48 to 72 h, matching results previously reported (1). The *sod-2* and *sod-3* mutants both showed larval arrest from the L3 to L4 stage that lasted longer than N2 (beyond 72 h) in Table 1. In Table 2, the *sod-2/3* mutants showed larval arrest at L3 at 72 h, while N2 and *sod-1/4/5* developed beyond L3 at this time point.

3.2 Growth Assay

The images in Figure 3 show that nematodes are straight after freezing for measurement in the microscopy field.

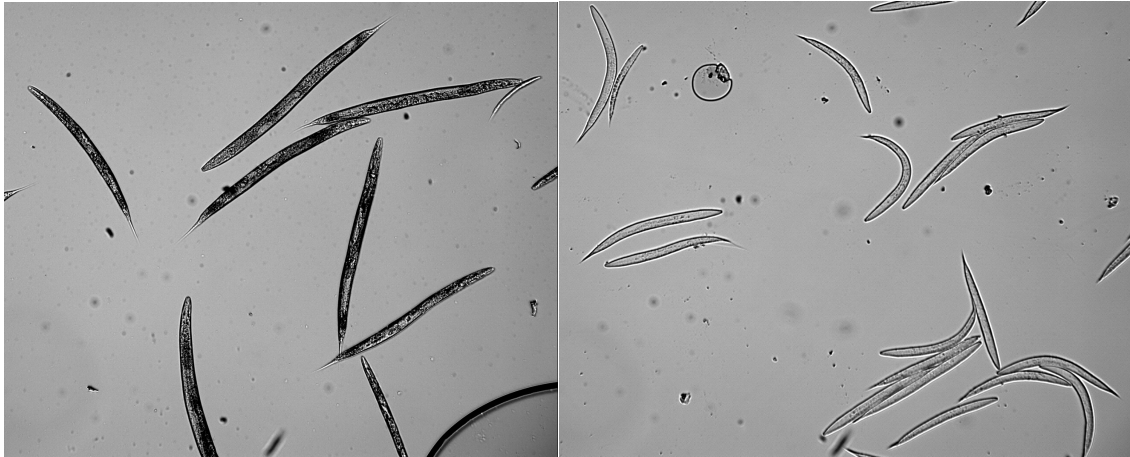


Figure 3. Examples of the microscopy images as used for growth measurements

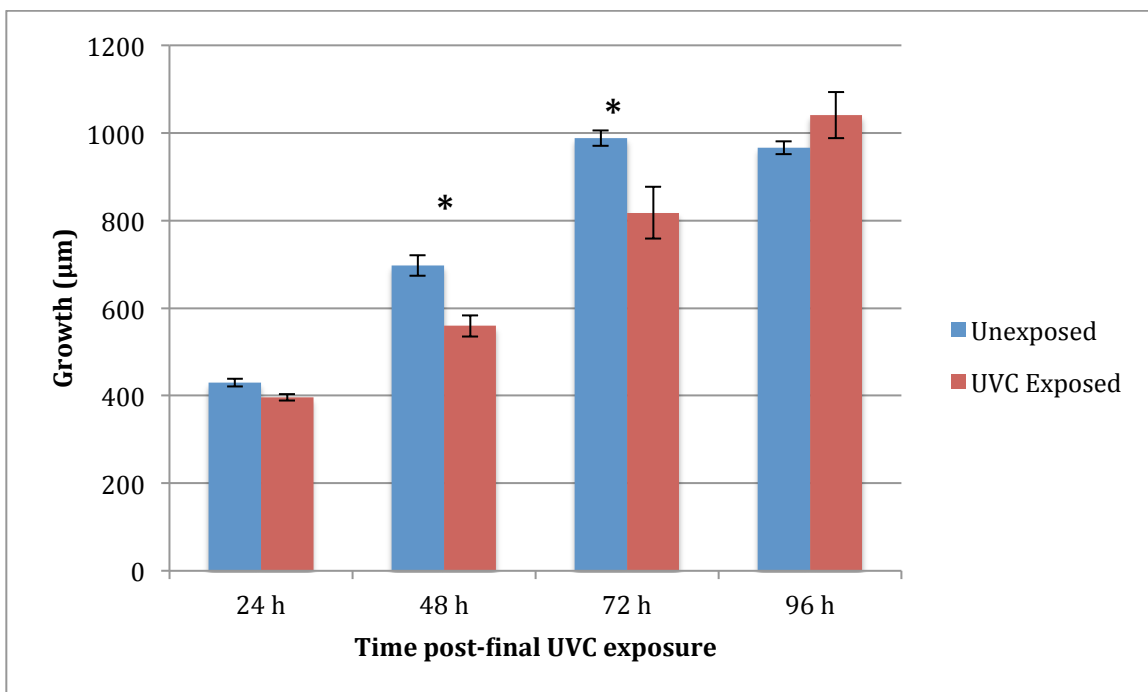


Figure 4. Growth of N2 after three consecutive exposures to 7.5 J/m² UVC (n = 15).

***Indicates statistically significant difference between unexposed control and UVC at $\alpha = 0.05$.**

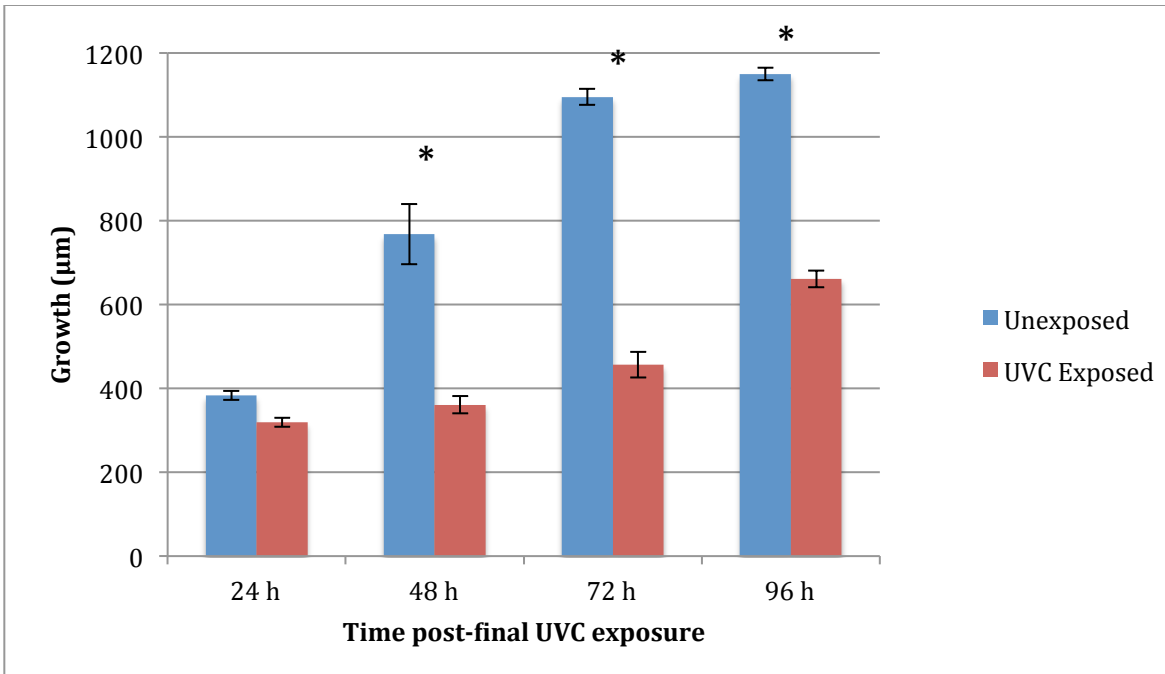


Figure 5. Growth of *sod-2* after 3 exposures to 7.5 J/m² UVC (n = 15).

***Indicates statistically significant difference between unexposed control and UVC at $\alpha = 0.05$.**

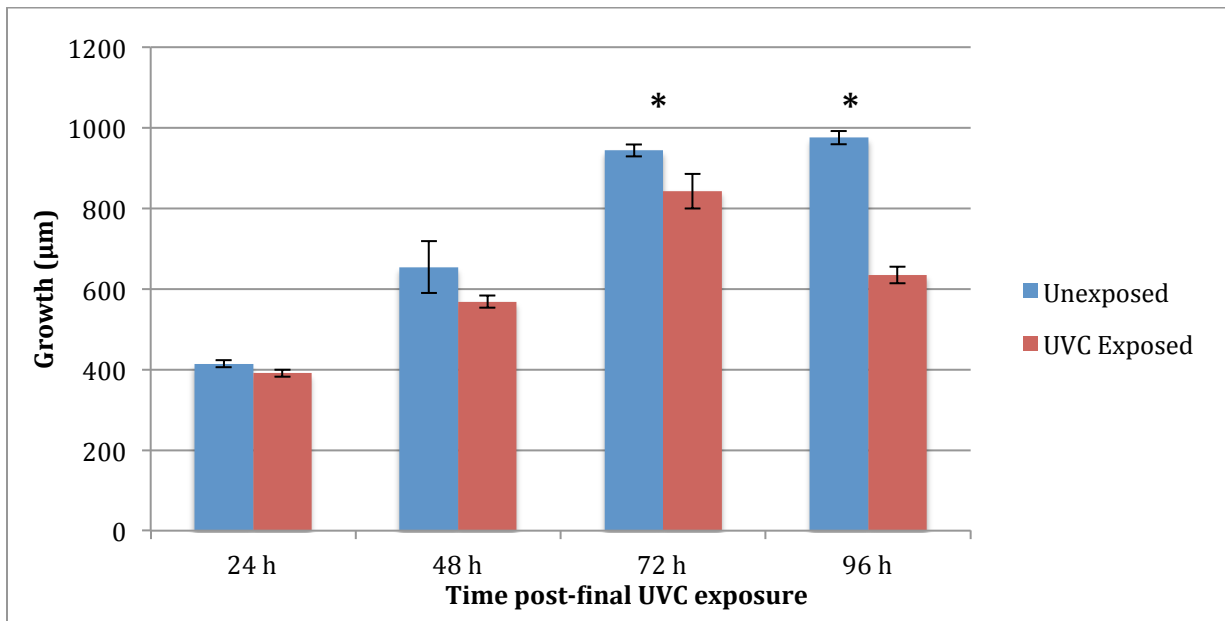


Figure 6. Growth of *sod-3* after 3 exposures to 7.5 J/m² UVC (n = 15). *Indicates statistically significant difference between unexposed control and UVC at $\alpha = 0.05$.

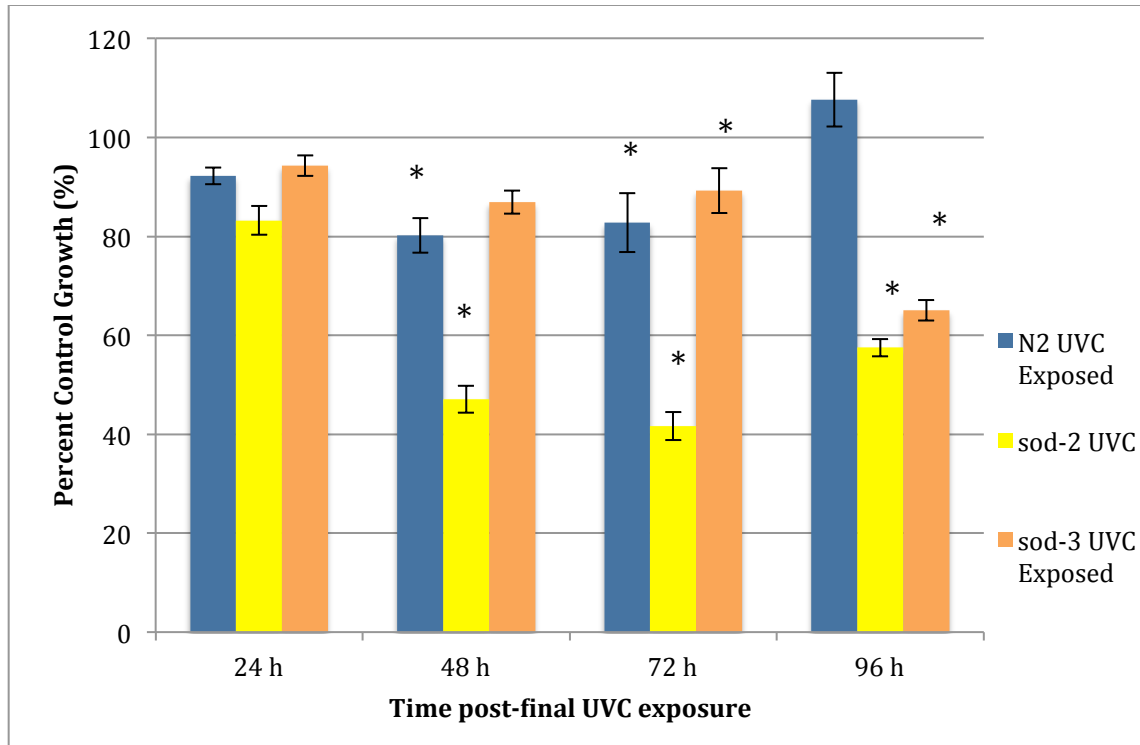


Figure 7. Percent unexposed control growth of N2, *sod-2*, and *sod-3* after 3 exposures to 7.5 J/m² UVC (n = 15).

***Indicates statistically significant difference between unexposed control and UVC at $\alpha = 0.05$.**

Using the data presented in Figures 4, 5, and 6, three-factor ANOVA test for all three strains showed global ANOVA significance ($p < 0.001$). Two-factor ANOVA tests for each strain showed significant interactions between exposure and time for all strains. Post-hoc Tukey analysis within each strain a significant effect of UVC on N2 growth at 48 h; *sod-2* at 48, 72, and 96 h; *sod-3* at 72 and 96 h. Two-factor ANOVA tests using the percent unexposed control data in Figure 7 comparing N2 and *sod-2* showed a statistically significant interaction between time and strain ($p < 0.001$) with a significant difference between N2 and *sod-2* percent unexposed control growth at 48, 72, and 96 h (all times $p < 0.0001$). Two-factor ANOVA tests using the percent unexposed control data comparing N2 and *sod-3* showed a statistically significant interaction

between time and strain ($p < 0.001$) with a significant difference between N2 and *sod-2* percent unexposed control growth at 96 h ($p < 0.0001$). The data in Figures 4-7 show increased growth inhibition in both *sod-2* and *sod-3* compared to N2 with greater inhibition in *sod-2* than in *sod-3*.

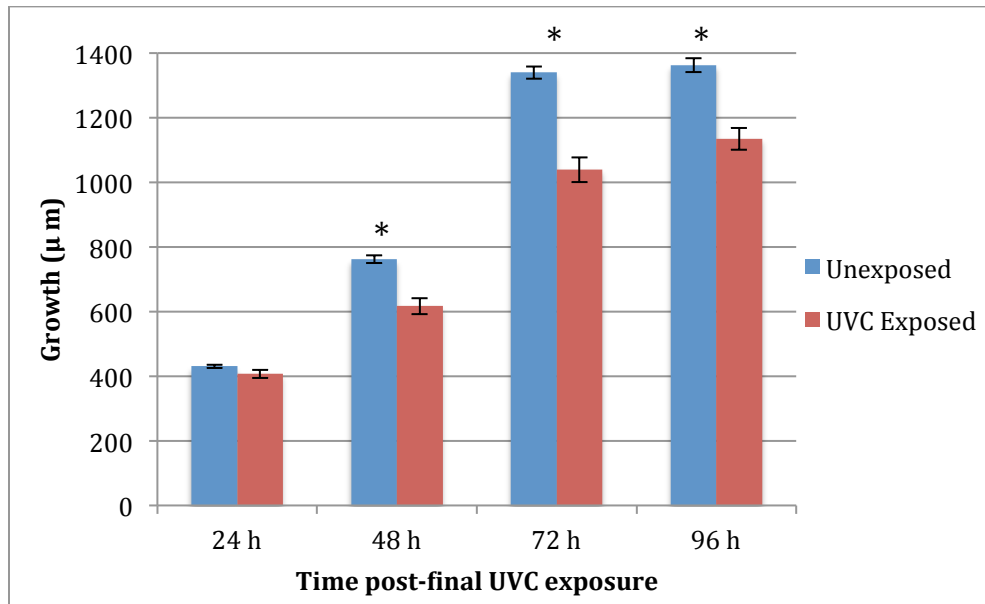


Figure 8. N2 growth after three consecutive exposures to 7.5 J/m^2 UVC ($n = 20$).

***Indicates statistically significant difference between unexposed control and UVC at $\alpha = 0.05$.**

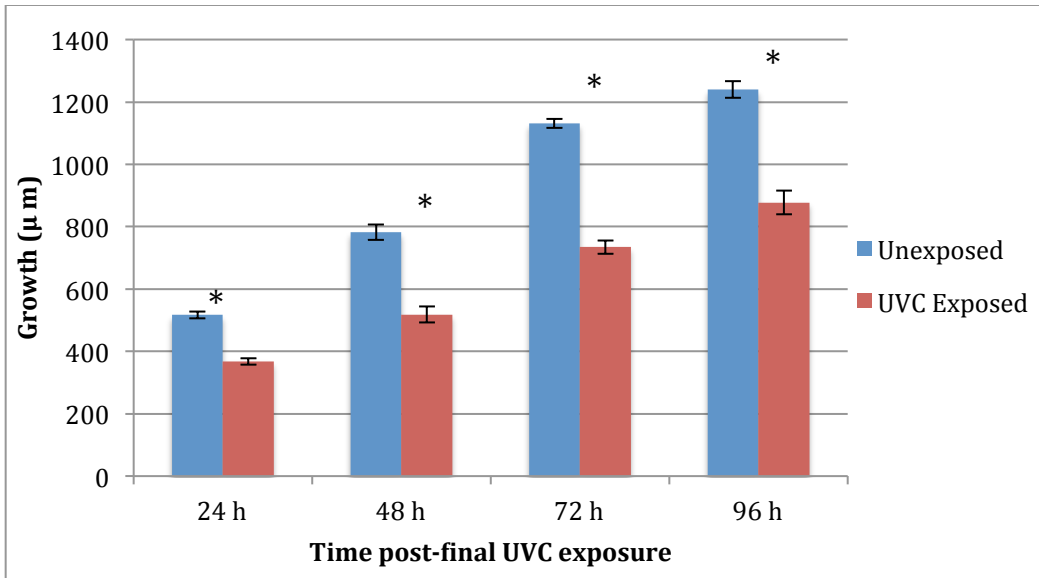


Figure 9. *sod-2/3* growth after three consecutive exposures to 7.5 J/m² UVC (n = 20).

***Indicates statistically significant difference between unexposed control and UVC at $\alpha = 0.05$.**

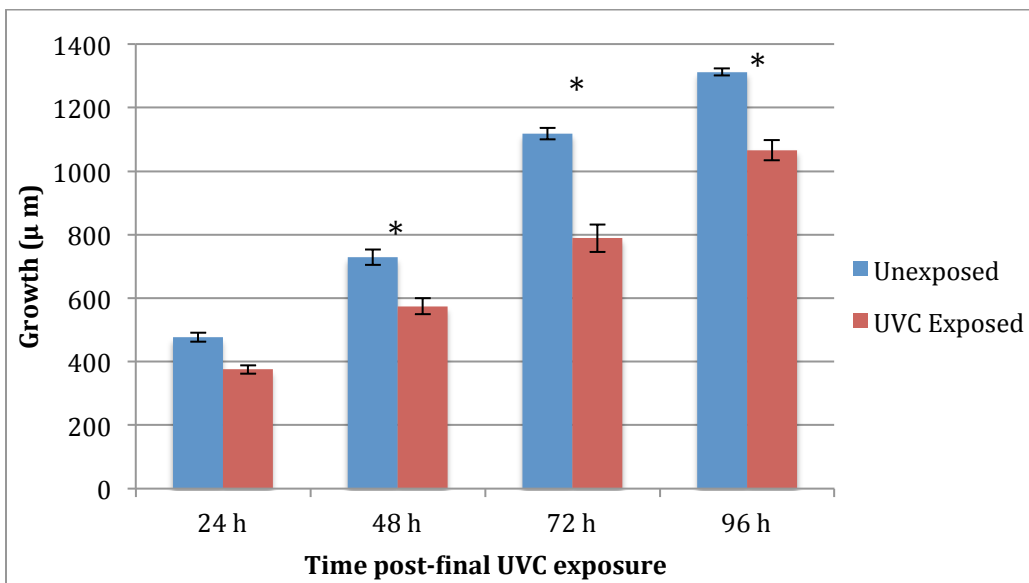


Figure 10. *sod-1/4/5* growth after 3 exposures to 7.5 J/m² UVC (n=20).

***Indicates statistically significant difference between unexposed control and UVC at $\alpha = 0.05$.**

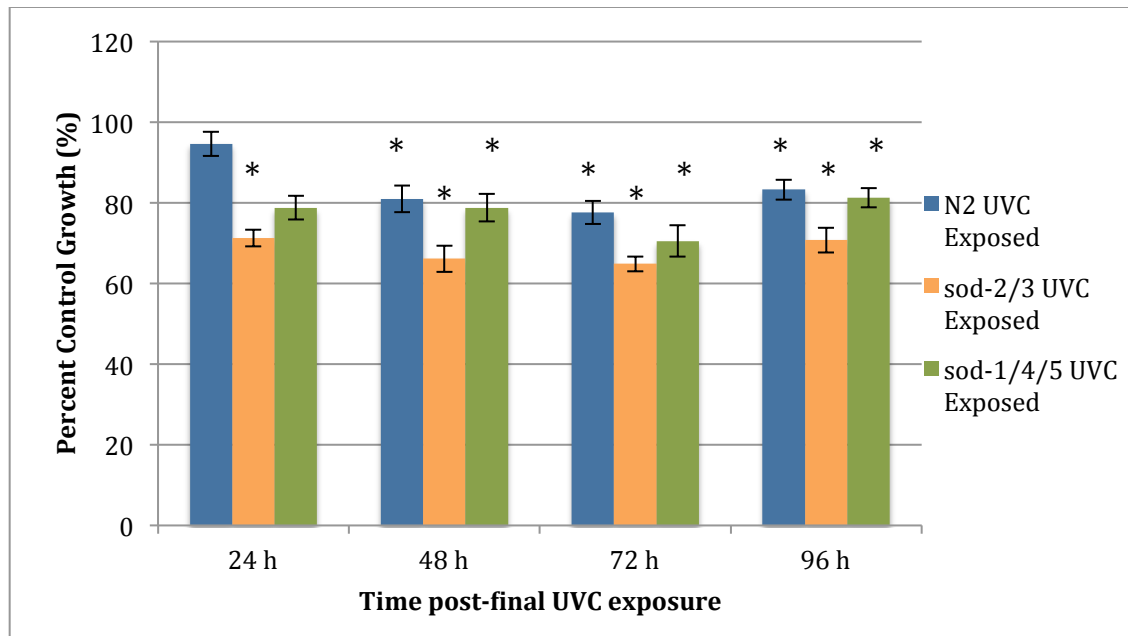


Figure 11. Percent unexposed control growth of N2, *sod-2/3*, and *sod-1/4/5* after 3 exposures to 7.5 J/m² UVC (n = 20).

***Indicates statistically significant difference between unexposed control and UVC at $\alpha = 0.05$.**

Using the data presented in Figures 8, 9, and 10, three-factor ANOVA test showed significance ($p < 0.001$) between N2, *sod-2/3*, and *sod-1/4/5* growth results for an interaction between strain and exposure, strain and time, exposure and time, but not all three factors ($p = 0.9209$). Three-factor ANOVA for N2 and *sod-2/3* showed significant interactions between strain and exposure, exposure and time, and strain and time (all $p < 0.001$), but this could not be further investigated due to lack of global ANOVA significance ($p = 0.9479$). Two-factor ANOVA tests for each strain showed significant interactions between exposure and time for all strains. In post-hoc Tukey analysis within each strain, N2 nematodes showed UVC irradiation has a significant effect on growth at 48, 72, and 96 h; *sod-2/3* at all time points; *sod-1/4/5* at 48, 72, and 96 h.

Two-factor ANOVA tests using the percent unexposed control data presented in Figure 11 comparing N2 and *sod-2/3* showed statistically significant effects of time and strain, but not a significant interaction between strain and time ($p = 0.1681$). Two-factor ANOVA tests using the percent unexposed control data comparing N2 and *sod-1/4/5* also did not show a significant interaction between strain and time ($p = 0.0868$).

3.3 Mitochondrial and Nuclear Genome Copy Number

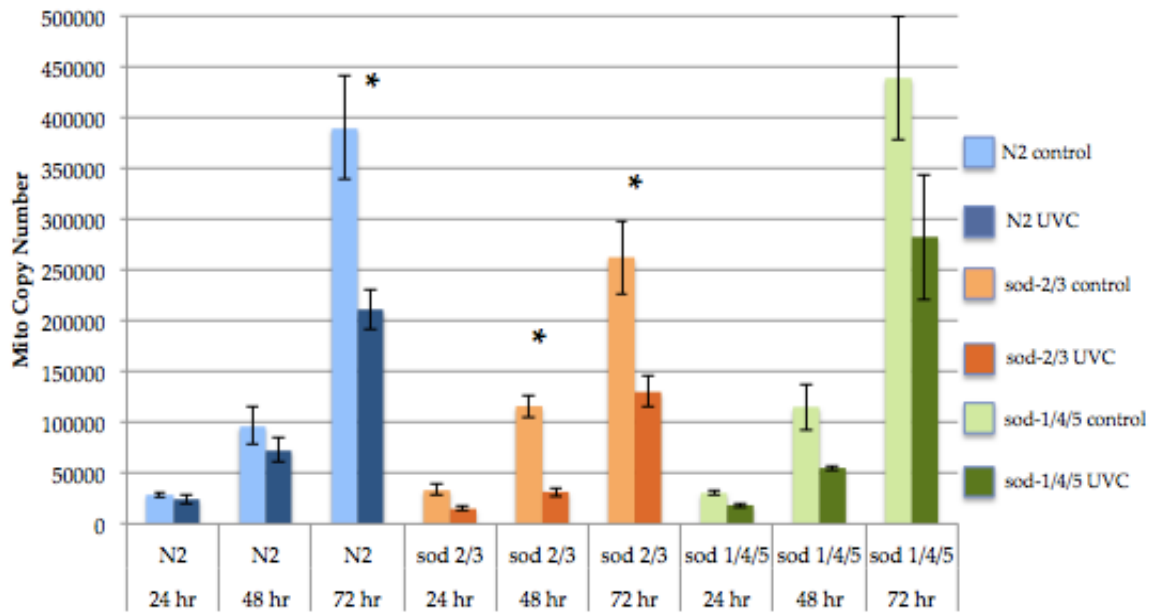


Figure 12. Mitochondrial copy number for *N2*, *sod-2/3*, and *sod-1/4/5* (n = 9 for 24 and 48 h; n = 6 for 72 h).

***Indicates statistically significant difference between unexposed control and UVC at $\alpha = 0.05$.**

For the mitochondrial copy number data presented in Figure 12, three-factor ANOVA test for all three strains showed significant interactions between strain and time/exposure and time, but not for strain and exposure ($p = 0.9359$) nor global significance ($p = 0.6505$). Two-

factor ANOVA tests for each strain showed significant interactions between exposure and time for all strains. Post-hoc Tukey analysis on each strain showed a significant effect of UVC on N2 at 72 h ($p < 0.001$), *sod-2/3* at 48 and 72 h ($p = 0.0025$ and $p \leq 0.001$, respectively), but not for *sod-1/4/5* at an identifiable time point ($p = 0.0831$ for interaction between exposure and time). The significant effect of UVC on N2 and *sod-1/4/5* copy number is lost when 72 h is not considered.

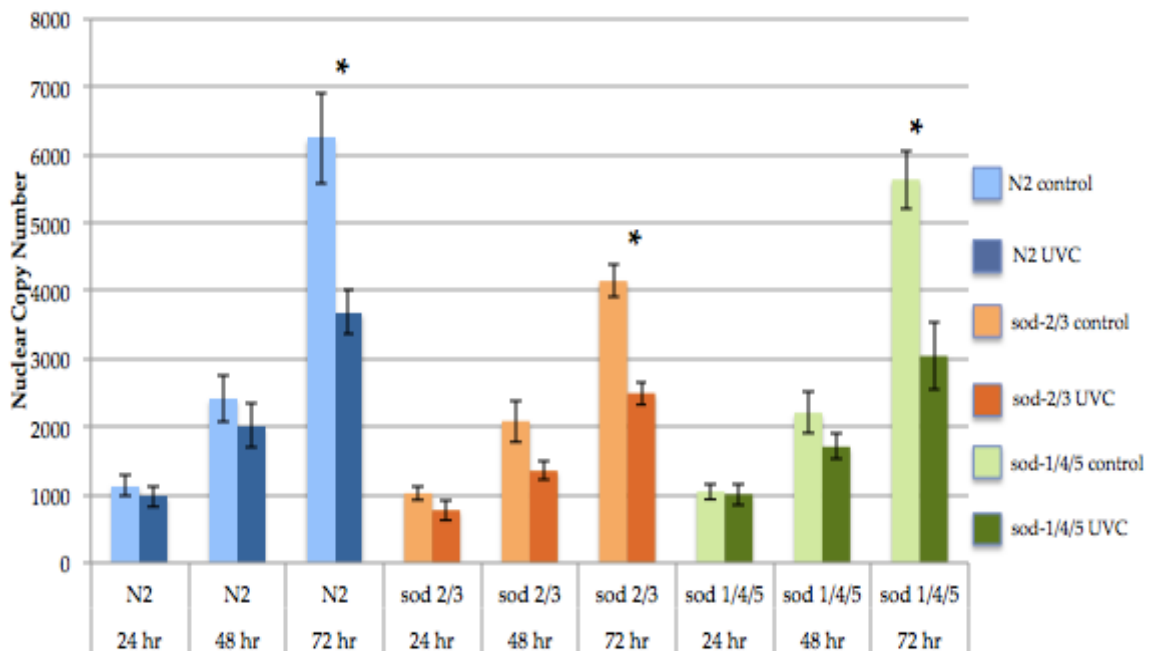


Figure 13. Nuclear copy number for *N2*, *sod-2/3*, and *sod-1/4/5* (n = 9 for 24 and 48 hours; n = 6 for 72 hours).

***Indicates statistically significant difference between unexposed control and UVC at $\alpha = 0.05$.**

For the nuclear copy number data presented in Figure 13, the three-factor ANOVA test for all three strains showed significant interactions between strain and time/exposure and time, but not for strain and exposure ($p = 0.8468$) nor global significance ($p = 0.4938$). Two-factor

ANOVA tests for each strain showed significant interactions between exposure and time for all strains. Post-hoc Tukey analysis on each strain showed a significant effect of UVC on N2 at 72 h ($p \leq 0.0003$), *sod-2/3* at 72 h ($p \leq 0.001$), and *sod-1/4/5* at 72 h ($p < 0.001$). The significant effect of UVC on N2 and *sod-1/4/5* copy number is lost when 72 h is not considered.

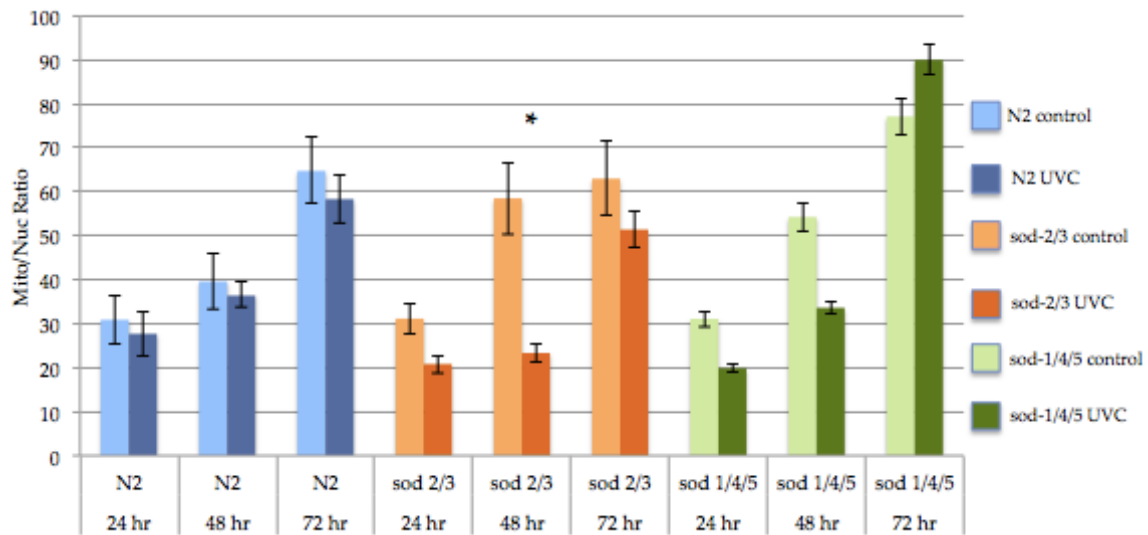


Figure 14. Mitochondrial-to-nuclear copy number ratio for *N2*, *sod-2/3*, and *sod-1/4/5* (n = 9 for 24 and 48 h; n = 6 for 72 h).

***Indicates statistically significant difference between unexposed control and UVC at $\alpha = 0.05$.**

For the mitochondrial-to-nuclear copy number ratio presented in Figure 14, three-factor ANOVA test for all three strains showed significant interactions between strain and time/exposure and time/strain and exposure (although borderline at = 0.0489), but not global significance ($p = 0.1017$). Two-factor ANOVA tests for each strain showed significant interactions between exposure and time for *sod-2/3* and *sod-1/4/5*, but not N2 ($p = 0.9539$). Post-

hoc Tukey analysis on each strain showed a significant effect of UVC on *sod-2/3* at 48 h ($p = 0.0005$), but not *sod-1/4/5* at any time points.

3.4 Heat Shock Protein Gene Expression

3.4.1 *hsp-6* Gene Expression

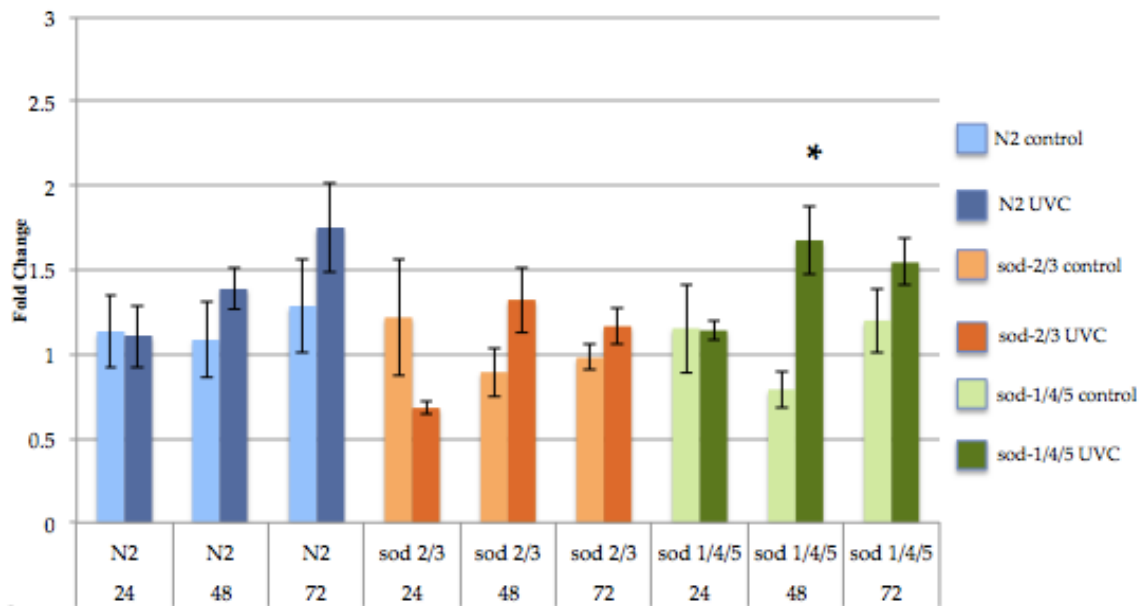


Figure 15. Gene expression for mitochondrial *hsp-6*.

***Indicates statistically significant difference between unexposed control and UVC at $\alpha = 0.05$.**

For the data presented in Figure 15, three-factor ANOVA tests including all strains did not indicate global ANOVA significance. Two-factor ANOVA tests for each strain individually showed a significant interaction between exposure and time for *sod-1/4/5* only ($p = 0.0483$).

Post-hoc Tukey analysis further defined this significant effect of UVC on *sod-1/4/5* at 48 h ($p = 0.0212$).

3.4.2 *hsp-60a* Gene Expression

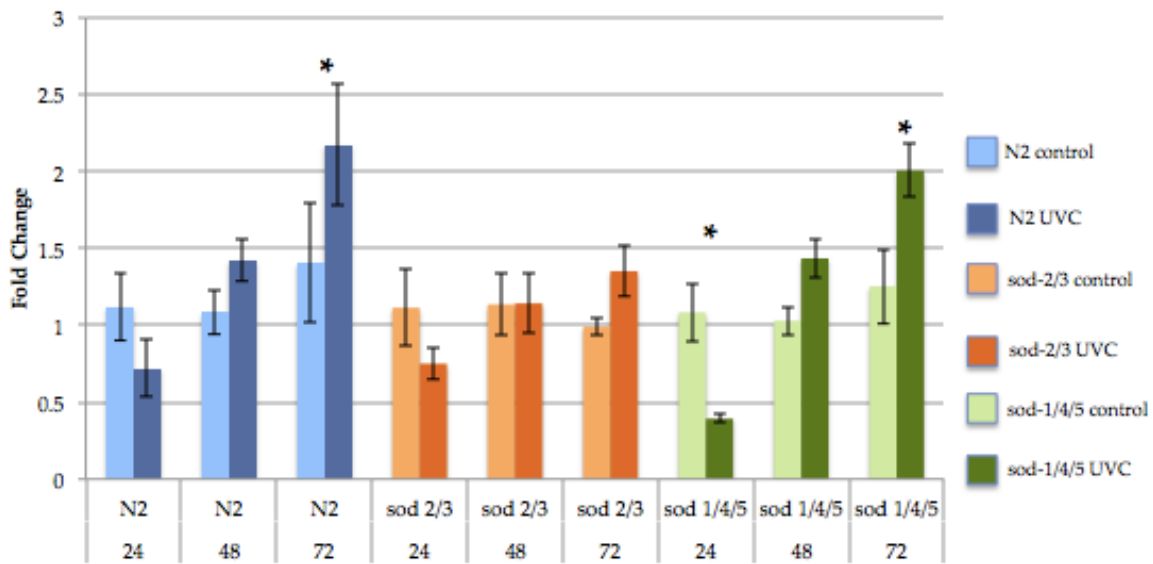


Figure 16. Gene expression for mitochondrial *hsp-60a*.

***Indicates statistically significant difference between unexposed control and UVC at $\alpha = 0.05$.**

For the data presented in Figure 16, three-factor ANOVA test for all strains did not indicate global ANOVA significance. Two-factor ANOVA tests for each strain showed a significant interactions between exposure and time for N2 and *sod-1/4/5* ($p = 0.007$ and $p < 0.001$), but not *sod-2/3*. Post-hoc Tukey analysis showed a significant effect of UVC on N2 at 72 h ($p = 0.011$) and *sod-1/4/5* at 24 h ($p = 0.0154$) and 72 h ($p = 0.0025$).

3.4.3 *hsp-60b* Gene Expression

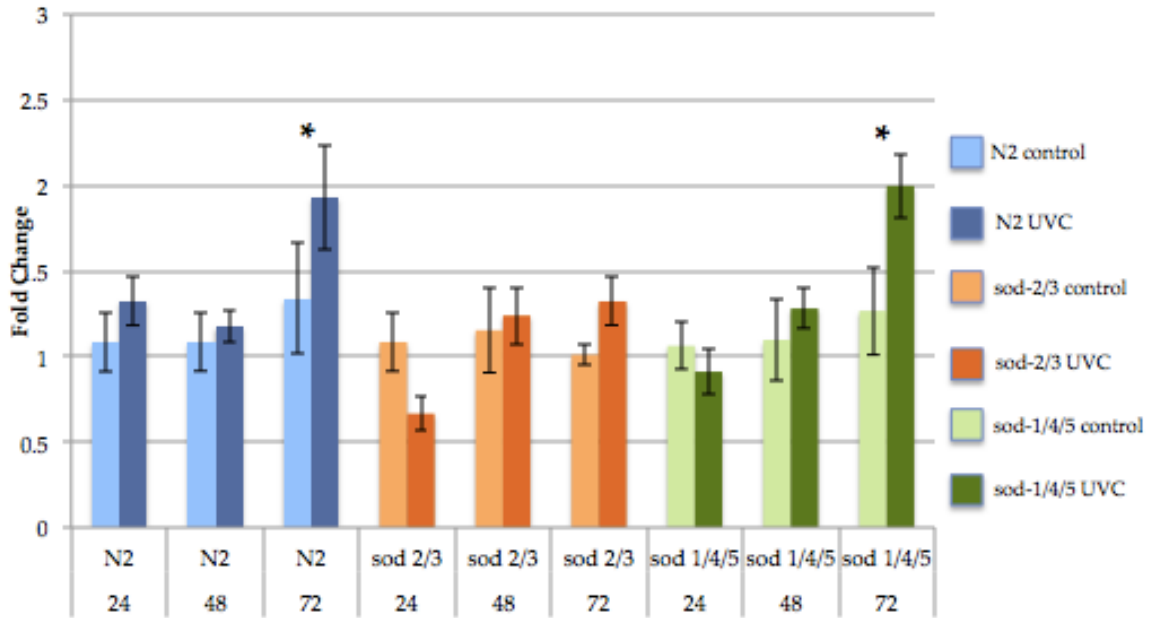


Figure 17. Gene expression of mitochondrial *hsp-60b*.

***Indicates statistically significant difference between unexposed control and UVC at $\alpha = 0.05$.**

For the data presented in Figure 17, three-factor ANOVA test for all strains did not indicate global ANOVA significance. Two-factor ANOVA tests for each strain showed a significant interactions between exposure and time for N2 and *sod-1/4/5* ($p = 0.0113$ and $p = 0.007$), while *sod-2/3* has borderline significance ($p = 0.0706$). Post-hoc Tukey analysis showed a significant effect of UVC on N2 at 72 h ($p = 0.0038$) and *sod-1/4/5* at 72 h ($p = 0.0075$).

3.4.4 *hsp-4* Gene Expression

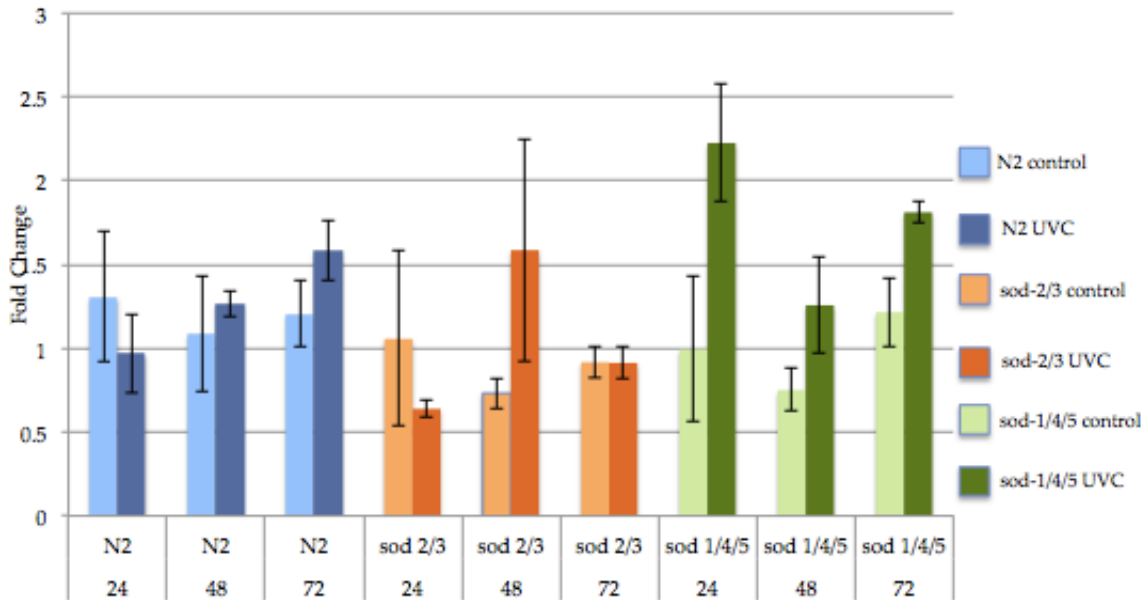


Figure 18. Gene expression of endoplasmic reticulum *hsp-4*.

For the data presented in Figure 18, three-factor ANOVA test for all strains did not indicate global ANOVA significance. Two-factor ANOVA tests for each strain did show significant interactions between exposure and time for any strain. Only *sod-1/4/5* showed significant effect of UVC when averaged across all time points ($p = 0.0482$), but N2 and *sod-2/3* did not ($p = 0.3635$ and $p = 0.6188$, respectively).

3.4.5 *hsp-16.2* Gene Expression

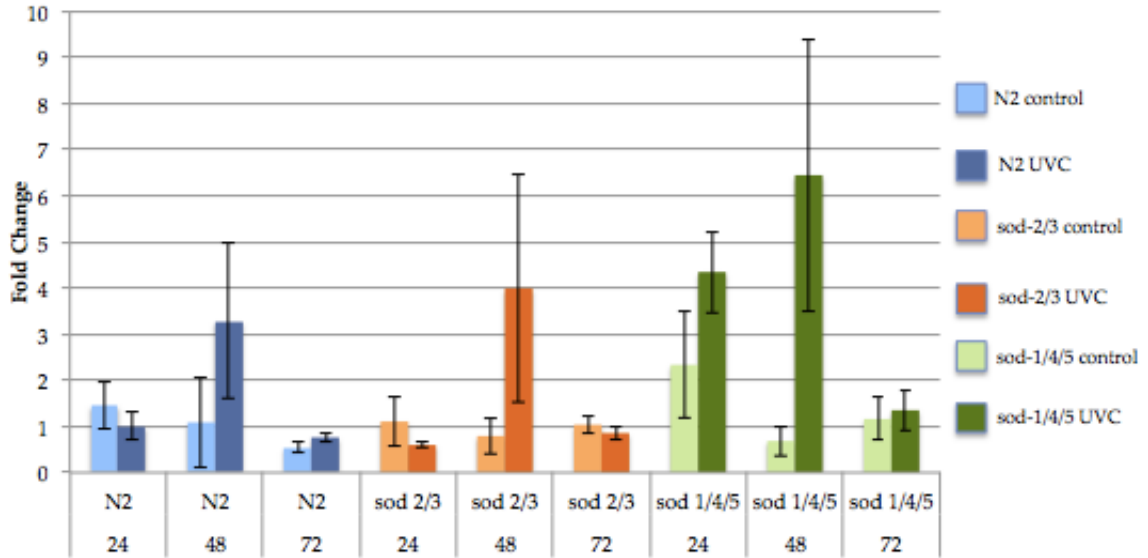


Figure 19. Gene expression of cytosolic *hsp-16.2*.

For statistical analyses of the data presented in Figure 19, the 48 h time point data was excluded due to high variability in all strains for both exposed and unexposed data. The raw data reflects a pattern of *hsp-16.2* gene expression decreases with each addition experiment replicate (three in total) among all strains at 48 h. Three-factor ANOVA test for all strains did not indicate global ANOVA significance. Two-factor ANOVA tests for each strain did show significant interactions between exposure and time nor a significant effect of UVC for any strain.

3.4.6 *hsp-16.41* Gene Expression

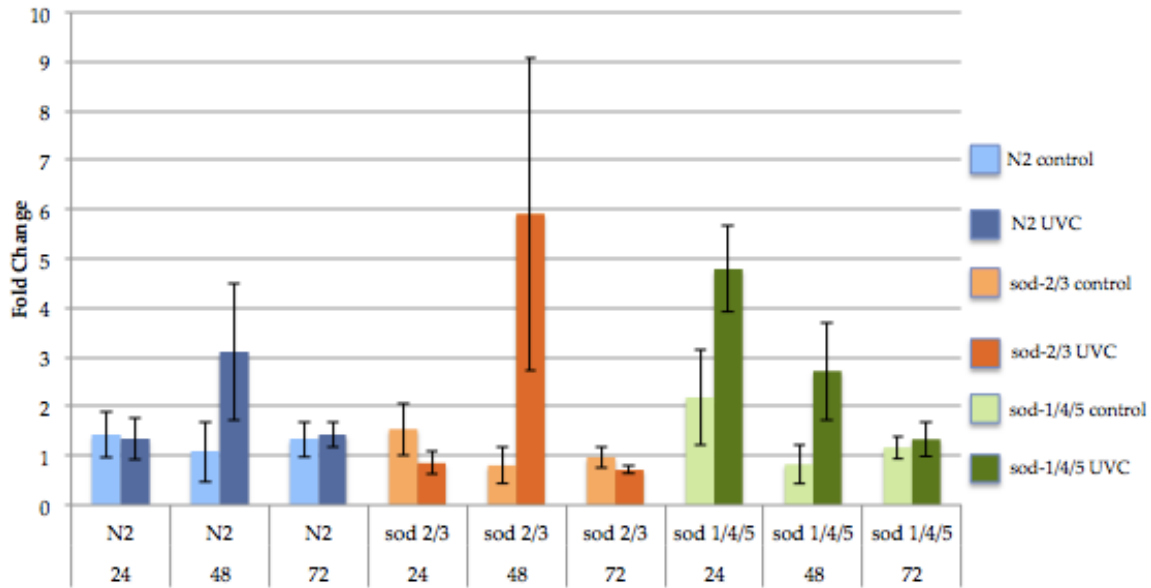


Figure 20. Gene expression of cytosolic *hsp-16.41*.

For statistical analyses of the data presented in Figure 20, the 48 h time point data was excluded due to high variability in all strains for both exposed and unexposed data. The raw data reflects a pattern of *hsp-16.41* gene expression decreases with each addition experiment replicate (three in total) among all strains at 48 h. Three-factor ANOVA test for all strains did not indicate global ANOVA significance. Two-factor ANOVA tests for each strain did show significant interactions between exposure and time nor a significant effect of UVC for any strain.

3.5 DNA Damage

During cycle optimization of samples for long amplicon quantitative PCR, fractional amplification reactions did not fluoresce with PicoGreen in acceptable fractional values. Optimal cycle numbers were concluded as 27 cycles for 24 and 26 cycles for 48 h based on acceptable values for 100% template QPCR amplification. QPCR reactions were not performed with UVC-exposed samples.

Table 3. Mitochondrial Long Amplicon Fractional Amplification PicoGreen Fluorescence.

Values are shown for two biological replicates of unexposed controls. Standard errors of averaged technical replicates were large, highlighting high variability between fluorescent readings. Data is not shown for nuclear damage cycle optimization; results similarly variable .

Strain, Hours post-final UVC exposure	50% template amplification	25% template amplification	12.5% template amplification
N2, 24 h	0.2797, 0.3363	0.1558, 0.1493	0.0916, 0.1210
<i>sod-2/3</i> , 24 h	0.3494, 0.3042	0.2104, 0.1976	0.1382, 0.1138
<i>sod-1/4/5</i> , 24 h	0.2640, 0.2844	0.1618, 0.1652	0.1044, 0.1005
N2, 48 h	0.3355, 0.1249	0.1258, 0.0824	0.0851, 0.0521
<i>sod-2/3</i> , 48 h	0.5545, 0.6998	0.3113, 0.3046	0.2097, 0.1301
<i>sod-1/4/5</i> , 48 h	0.5416, 0.2659	0.3332, 0.1037	0.1932, 0.0482

4. DISCUSSION

4.1. Larval Arrest Screening

The longer arrest for *sod-2* larvae compared to *sod-3* larvae is likely explained by the difference in expression levels for the two genes, with *sod-2* encoding the major MnSOD protein (at ~90% of total MnSOD) and *sod-3* encoding the minor MnSOD protein (25). The *sod-3* mutants are expected to be less sensitive to mitochondrial ROS than *sod-2* because *sod-3* is the minor MnSOD (25). It has also been reported that deletion of one MnSOD gene does not cause a significant increase in the level of expression of the other MnSOD gene, suggesting that more significant arrest in *sod-2* compared to *sod-3* is not confounded by a compensatory upregulation of the other MnSOD (26). As stated, this observed developmental arrest was considered preliminary evidence of ETC dysfunction since OXPHOS is necessary for the transition from L3 to L4 (7), and these results prompted the further study of mitochondrial ROS from persistent mtDNA as a mechanism contributing to ETC dysfunction.

The stage-scoring results presented in Table 2 show that the *sod-2/3* mutants are temporarily arrested in the L3 stage compared to unexposed control and wild-type exposed groups. However, they were not more delayed in development compared to *sod-2* and *sod-3* mutants as hypothesized and were actually less delayed compared to *sod-2*. This could be explained by reported increases in the gene expression of other antioxidant and detoxification genes in *sod-2/3* mutants including five different glutathione-S-transferase genes that detoxify xenobiotics and *cyp-13* that regulates DNA degradation and cell death (26). The *sod-1/4/5* UVC-exposed nematodes showed a slight delay in development during the first 48 to 72 h compared to *sod-1/4/5* unexposed controls with a slight arrest at the L3 stage. However, the observable delay disappeared by 72 h. The *sod-1/4/5* UVC-exposed nematodes were not significantly delayed in

comparison to N2 nematodes exposed to UVC, but were significantly less delayed compared to the *sod-2/3* nematodes exposed to UVC. These results match the hypothesis that *sod-2/3* would be more arrested than N2, but *sod-1/4/5* would not, and suggest that there may not be an increase in ETC dysfunction or other activated developmental delay mechanisms resulting from decreased defenses to cytosolic ROS after exposure to UVC.

The inconsistency between the N2 unexposed control and UVC-exposed developmental stage scoring results reported in Table 1 and Table 2 (with N2 UVC-exposed nematodes progressing more quickly; Table 2) is likely explained by normal variation in nematode development and matches the variation between the reported growths of each group. Increasing the sample size could reduce this variation between the sets of experiments.

4.2 Growth

Growth measurement results showed growth inhibition due to UVC exposure in all strains, matching previously reported data in N2 (7). The growth *sod-2* and *sod-3* mutants was inhibited and statistically different from same-strain unexposed controls and from N2 when the data was analyzed as percent growth of unexposed control. The increased sensitivity of *sod-2* mutants to UVC exposure compared to *sod-3* is again seen with *sod-2* growth being significantly different from wild-type as percent growth of unexposed control at 48, 72, and 96 h compared to only at 96 h in *sod-3*.

The variability in the N2 growth results between the data presented in Figure 4 and Figure 8 is likely due to a small sample size and a slight variation between experiments, which is expected. This difference matches the differences seen in N2 development data presented in Table 1 and Table 2.

The *sod-2/3* growth measurements showed that growth was inhibited after UVC exposure, but differences from N2 at specific time points could not be investigated due to the lack of a significant interaction between strain and time when compared in a two-factor ANOVA analysis as explained in section 3.5. The lower percent-unexposed control growth for *sod-2* compared to *sod-2/3* matches the longer developmental delay in development observed in the *sod-2* samples compared to *sod-2/3*. The significant difference between *sod-2* or *sod-3* and N2 but not between *sod-2/3* and N2 may be due to the variation between the two sets of N2 data from the separate experiment sets. The similar results for N2 and *sod-1/4/5* growth match the similarity observed in the development assay in Table 2, suggesting that the UVC exposure is not inducing changes to the extracellular and cytosolic ROS levels that cause growth inhibition different from wild-type growth comparisons.

A relationship between growth and development is understood, as *C. elegans* increase in size dramatically between larval and adult stages. Comparisons between the results and conclusions of the development and growth analyses match in significance with respect to UVC effects and mutant to wild-type comparisons.

4.3 Mitochondrial and Nuclear Genome Copy Number

Leung *et al.* (2013) reported a significant effect of UVC exposure on mtDNA copy number in *glp-1* mutant nematodes that lack a functioning germ-line when cultured at 25°C (7). In this project, all strains tested were expected to show a decrease in mitochondrial copy number as the *glp-1* results suggested (7); *sod-2/3* copy number was expected to be lower than N2 and *sod-1/4/5*. The results support only the latter hypothesis of decreased mitochondrial copy number, suggesting that UVC exposure may decrease mtDNA replication and/or lead to mitochondrial

degradation as a result of increased mitochondrial superoxide levels (assumed from decrease in MnSOD defenses), but not from increased cytosolic superoxide anion levels. If Leung *et al.* (2013) had not reported a decrease in mtDNA copy number, we could have hypothesized that mtDNA copy number increases due to UVC exposure as a compensatory reaction (7).

UVC exposure was expected to statistically decreased N2 and *sod-1/4/5* mitochondrial copy number, but this was only the case at 72 h. At 72 h, unexposed control nematodes had reached reproductive maturity while UVC-exposed nematodes generally did not show gravidity or lay eggs. Although measuring rate of reproduction was not an aim of this project, observations were made about the rates of egg-laying rates between N2, *sod-2/3*, and *sod-1/4/5*. Compared to N2, *sod-2/3* were observed to, on average, lay fewer eggs on average than N2 (and also on average 4-8 h later) while *sod-1/4/5* were observed to lay the same number of eggs if not more. While this reproductive data is only based on visual observations and not quantitative measurements, similar outcomes have been reported (24). Unexposed control group copy number measurements were confounded by amplification of the genomes in eggs, and there is an effect-measure modification of genome copy number at 72 h between unexposed control and UVC-exposed of the same strain. The lack of significance at earlier time points suggests that UVC exposure is not changing mitochondrial copy number and/or is not resulting in increased cytosolic ROS that alters mtDNA copy number. The difference in effect of UVC exposure in N2 and *sod-1/4/5* compared to *glp-1* also suggests that a functioning germ-line may help sustain or recover mtDNA copy number after mtDNA damage even before reproduction starts at 72 h.

The lack of a significant effect of UVC exposure on nDNA copy number at time points other than 72 h (again increased by reproduction in the unexposed controls) suggests that this level of persistent mtDNA damage does not impact cellular division. It also indicates that

decreased defenses to superoxide in neither mitochondrial nor the cytosol have no additional effect on nDNA copy number, and is consistent with results reported previously (7).

When represented as mitochondrial-to-nuclear genome copy number ratio, the data is normalized for differences in cell size and cell number and therefore, the data is controlling for the genomes in eggs. As copy number ratios, only the *sod-2/3* at 48 h data was statistically affected by UVC exposure. This result suggests that antioxidant defenses to mitochondrial superoxide are necessary to maintain mtDNA copy number and likely suggest that mitochondrial superoxide is increased as a result of UVC exposure. One possible mechanism contributing to this change in *sod-2/3* mtDNA copy number could be oxidation of pol γ , the mitochondrial DNA polymerase. This is supported by a study in which human fibroblasts resulted in decreased mitochondrial copy number due to oxidation of pol γ from exposure to H₂O₂ (27). There may also be altered or insufficient cellular signaling regarding mitochondrial genome replication and pol γ activity, such as is the case with mitochondrial transcription factor A that signals for pol γ upregulation under oxidative stress conditions in human fibroblasts (28, 29). However, the signaling mechanisms of pol γ conditions of oxidative stress in *C. elegans* are not as well understood (7).

Additionally, the developmental stage of the nematodes at these measured time points may be influencing the biological need for mitochondrial copy number. Prior to activation of OXPHOS at the L4 larval stage, the rates of mitochondrial genome are not as high as during the L4 stage because the proteins it encodes are not yet needed. The longer arrest at L3 before progression to L4 seen in Table 2 for *sod-2/3* UVC-exposed nematodes compared to N2 supports this idea. Further study is warranted to understand the levels of gene transcription for pol γ could help explain this observation.

4.4 Heat Shock Protein Gene Expression

4.4.1 Mitochondrial hsp gene expression (*hsp-6*, *hsp-60a*, *hsp-60b*)

I hypothesized that the persistent mtDNA damage resulting from UVC exposure would result in an upregulation of hsp genes encoding mitochondrial hsp. It was predicted that the mtDNA damage could induce a mitochondrial unfolded protein response UPR^{mt} if [1] damaged DNA did not allow for proper protein translation and folding (22), [2] if increased ROS from ETC dysfunction oxidized proteins (19, 30) causing them to unfold/improperly fold, or [3] imbalance in the stoichiometric balance between nuclear-encoded and mitochondria-encoded genes of the ETC left proteins lingering in the mitochondrial matrix (16). The *sod-2/3* mutant was expected to have increased upregulation from that of wild-type due to the decreased defenses to the oxidative damaging ability superoxide anions in the mitochondria.

The first proposed mechanism by which UVC irradiation could induce a UPR^{mt} response (damaged DNA does not allow for proper protein translation and folding), can be further understood when results from the DNA damage assay are complete. The second mechanism (increased ROS from ETC dysfunction oxidizes proteins, causing them to unfold/improperly fold) is supported by Yoneda et al. who reported that RNAi knockdown of mtDNA genes encoding for ETC complexes activates a UPR^{mt} response (31). They report that knockdown of genes encoding for ETC complexes I or IV induce a response, while knockdown of genes encoding for ETC complex II did not (complex III genes not reported). Altered activity of complexes I, III, and IV, but not complex II are reported to result in increased production of superoxide. Evidence for mechanism three (imbalance in the stoichiometric balance between nuclear-encoded and mitochondria-encoded genes of the ETC leave proteins lingering in the mitochondrial matrix) comes from Houtkooper et al.. They reported that the mitochondrial UPR

can be activated by “a stoichiometric imbalance between nDNA- and mtDNA-encoded oxidative phosphorylation proteins,” although the evidence for a specific pathway linking the two events was not reported (16). One possible explanation for this mechanism not related to ROS production could be that the imbalance results in abandoned nuclear-encoded or mitochondrial encoded proteins in the mitochondrial matrix. Signaling events between the mitochondria and nuclear transcription factors such mammalian nuclear respiratory factor-1 that regulate transcription of nuclear-encoded mitochondria proteins (through mitochondrial transcription factor A) could also be a factor, but this signaling has not been identified in *C. elegans* (7).

The lack of a significant difference between unexposed control and UVC-exposed nematodes (except at 72 h for N2 and *sod-1/4/5*) did not provide evidence of ETC dysfunction characterized by the proposed possible mechanisms of UPR^{mt} activation. The upregulation at 72 h for N2 and *sod-1/4/5* cannot be explained. It is possible that the UVC-exposed nematodes are experiencing the beginning of increased mitochondrial activity compared to unexposed controls at 72 h that results in an increased initial mitochondrial stress response because they are just moving forward from the L4 stage. The UPR^{mt} is reported to be most active during the L4 stage when the rate of mitochondrial genome replication is highest during development (33). Prior to the L3 to L4 transition, transcription of ETC proteins is reduced (6). Once this ETC translation increases at the L4 stage at 72 h, mtDNA damage due to UVC irradiation could result in UPR^{mt} activation by one of three events specified earlier in this section. Surprisingly, there was no statistically significant effect of UVC irradiation on mitochondrial hsp gene expressions in *sod-2/3*. As stated earlier, *sod-2/3* mutants exhibit upregulation of other antioxidant and detoxification genes compared to N2; these changes in stress response gene regulation in N2 could result in different regulation of the UPR^{mt}. Alternatively, the statistically significant

reduction in mitochondrial copy number or larval development delay seen in UVC-exposed *sod-2/3* could result a lower baseline of mitochondrial activity and, therefore, ETC dysfunction would have a lesser impact on the UPR^{mt} threshold (33).

Induction of the UPR^{mt} and hsp transcription are part of a series of cell signaling events that occur after a threshold of unfolded or lingering proteins is sensed in the matrix. This multi-step signaling pathway is not fully understood and may provide further understanding on induction of the UPR^{mt} (33).

4.4.2 Endoplasmic reticulum and cytosolic hsp gene expression

I hypothesized that no strains would show upregulation of the endoplasmic reticulum (ER)-localized hsp-4 as part of the endoplasmic reticulum unfolded protein response (UPR^{ER}). The UPR^{ER} is thought to be primarily induced when the ER attempts to fold mutated proteins that are encoded for by the nuclear genome and the unfolded or improperly folded proteins accumulate in the ER lumen (34). Mutated proteins are the result of DNA mutations that alter the sequence of amino acids of proteins encoded for by a mutated nDNA template. The nDNA damage resulting from UVC exposure or from increased cytosolic ROS is not expected to mutate nDNA to a degree where nDNA mutations would result in mutated proteins; the nDNA photodimers resulting from UVC and/or possible oxidative nDNA from increased cytosolic ROS are expected to be repaired by robust nDNA repair machinery. The results support this hypothesis, with *sod-1/4/5* as the only strain showing a statistically significant effect of UVC as seen in Figure 16. It is unsurprising that *sod-1/4/5* would be the only mutant to suggest unfolded proteins in the ER lumen because it is the most vulnerable to increased cytosolic nDNA damage or oxidative protein damage. Since oxidative damage resulting in hsp-4 upregulation would be a result of

UVC exposure rather than ETC dysfunction (ETC produced superoxide cannot cross the mitochondrial membrane), any upregulation would be expected to decrease over time as the damage is repaired and proteins are turned-over.

I hypothesized that all strains would show upregulation of the cytosolic hsp-16.2 and hsp-16.41 after UVC exposure due to the ability of UVC irradiation to increase ROS levels (35). The *sod-1/4/5* mutant was expected to be the most sensitive to cytosolic ROS. The results did not show statistically significant effect of UVC exposure on any strain. However, the results showed tremendous variation between experiment replicates and high standard errors when the real-time PCR hsp gene values were normalized to the house keeping genes. The cytosolic hsp is a sensitive indicator of stress and could have been induced differently by unintended laboratory stressors during experiment replicates. The data showed that with each additional experiment (three in total), the cytosolic hsp gene expression decreased in both unexposed control and UVC-exposed groups, suggesting decreased sensitivity of the nematodes over the two-month period of sample collection for gene expression experiments. It is also possible that a slight variation in the collection of samples at 24-hour time points could contribute to the variability, although this does not explain the pattern of decreased expression. Real-time PCR measurement of these genes conducted in a different laboratory also had high standard errors (Rachel Goldstein, Freedman laboratory, NIEHS), but a reason has not been explained. Although variable, together these non-mitochondrial hsp-gene expression results suggest that no significant oxidative damage occurs to proteins in the cytosol due to UVC exposure.

4.5 DNA Damage

I hypothesized that the variable and low amplification of the fractional template amounts used during cycle optimization is due to a loss of DNA template integrity from improper storage conditions of the lysates. However, that hypothesis does not explain why 100% template amplification reactions sometimes reached expected fluorescent PicoGreen values somewhat. The low amplification of 12.5% template amplification reactions may also be a result of noise of the assay obscuring measurements of already low template levels (although above the limit of detection).

While incomplete at this time, the DNA damage assay remains an important experiment in this study of ROS resulting from ETC dysfunction and UVC exposure. Oxidative damage to DNA could include oxidative damage to bases and sugar phosphates in addition to single or double-strand breaks (36, 37). In nDNA, nucleotide excision repair and base excision repair are expected to repair this damage, while only base excision repair can repair this damage in mtDNA. It is expected that the great majority of this oxidative damage would be repaired by base excision repair (36, 37). The long amplicon QPCR protocol for this assay has been reported to detect oxidative DNA damage in mitochondria (36, 38).

A previous study has shown that nuclear DNA damage is repaired in N2 nematodes by 48 h post-final UVC exposure using the same UVC exposure protocol described here, while mtDNA damage persists (1). This assay could provide evidence for the hypotheses that decreased defenses against mitochondrial superoxide in the *sod-2/3* mutants leads to increased oxidative mtDNA damage that can not fully be repaired with nucleotide excision repair and that decreased defenses against cytosolic superoxide in the *sod-1/4/5* mutants does not lead to

increased oxidative nDNA damage because it can be repaired more robustly than in mtDNA in addition to receiving protection from nucleoside histone protein packaging (36).

4.6 Future Directions

These results presented here have provided evidence to pursue many future experiments to build upon and expand the questions of how mitochondrial function or dysfunction results from persistent mtDNA damage and how increased ROS results from mtDNA damage and contributes to ETC dysfunction. Experiments to successfully complete the DNA damage assay and an additional growth assay replicate are currently being pursued.

Additionally, function of the electron transport chain could be assessed through measuring ATP levels and oxygen consumption. The results of these assays could be compared to previous data from experiments measured throughout life of N2 and *glp* mutant strains to further understand the effects of SOD deficiency (7). A luciferase assay kit can measure ATP levels in which ATP is quantified as a measure of the light emitted when luciferin reacts with oxygen in lysed nematode samples with luciferase (39). Oxygen consumption can be measured using a Seahorse Bioscience Extracellular Flux Analyzer (Seahorse Bioscience) or other methods (30).

Transcription level of the mtDNA polymerase γ could be relevant to the negative effect UVC has on mitochondrial copy number in mitochondrial ROS sensitive mutants. A previous study showed an ~8 fold increase in *polg-1* (the nuclear-encoded gene for polymerase γ) expression from 24 to 48 h after final UVC exposure. In this project, a significance decrease in mtDNA genome copy number was seen at 48 h and may be explained by decreased *polg-1* expression. Polymerase γ levels could be quantified by looking at the gene expression of *polg-1*.

This could be performed by mRNA extraction and cDNA quantification with real-time PCR as reported in this project.

Additionally, as mentioned previously, oxidation of polymerase γ could result from increased ROS from ETC dysfunction or UVC exposure. This oxidation could inhibit polymerase γ activity, leading to decrease mtDNA genome copy number. Report of quantification oxidation of polymerase γ has been found in treatment of human fibroblasts with H_2O_2 , but not in *C. elegans* (27). This procedure could likely be adapted for *C. elegans*.

The ability to quantify levels of superoxide anion ($O_2^{\cdot-}$) and other ROS (specifically H_2O_2) in the *sod* mutants could strengthen our understanding of the increased oxidative stress these mutants experience and the potential for oxidative damage. Levels of H_2O_2 are of particular interest in addition to levels of $O_2^{\cdot-}$ because I hypothesized that SOD deficiency in the mutants could result in lower H_2O_2 from decreased conversion of $O_2^{\cdot-}$. If this hypothesis is correct and H_2O_2 plays a significant role in cell signaling in a relevant pathway such as stress response (unknown), the signaling could be confounding factor, as is the upregulation of antioxidant and detoxification genes in *sod-2/3* mutants. Until ROS production is quantified, we are only able to assume increased ROS based on the decreased defense against superoxide anions present in MnSOD mutants, although increased levels of steady-state ROS has been detected in *sod-2* mutants (19, 20). Reports of ROS quantification also state experimental difficulty (20). MitoSOX fluorescent dye (Thermo Fisher Scientific Inc.) is selective to superoxide anions in mitochondria, while other dyes are sensitive to general ROS in cells (although possibly not superoxide) (20). Other measures of inferred ROS generation such as protein oxidative damage are interesting, but not sufficient to conclude ROS levels because other factors can affect protein oxidative damage such as protein turnover or altered regulation of ROS detoxification (20).

5. CONCLUSION

Collectively, the results of this project have shown that UVC exposure to nematodes created mitochondrial-specific effects, strengthening evidence of altered ETC function. While the use of the MnSOD mutants does not provide causation that these results are due to increased ROS production by the ETC, they do provide evidence to further test this hypothesis in future experiments. The results from the non-mitochondrial mutant analyses suggest that UVC irradiation can be used for the selective study of mitochondrial DNA damage/dysfunction in *C. elegans*. However, investigation of effects of UVC exposure other than the mtDNA studied should continue.

The pursuit to understand the mechanisms connecting persistent mtDNA damage and ETC function or dysfunction should be expanded as this topic is relevant to cancer, aging, diabetes, and hundreds of mitochondrial diseases. While some mitochondrial diseases result from mtDNA mutants of unknown origin or membrane depolarization, others are due to unexplained mitochondrial dysfunction. As we expand our knowledge of environmental toxicants and environmental exposures, we must specifically expand our knowledge about mitochondrial function and dysfunction. This will be necessary to identify mitochondrial toxicants and understand their potential multifaceted toxicological effects including persistent mtDNA damage and increased oxidative stress. Further investigation of this project's aims could provide for the knowledge needed to development treatments for mitochondrial disorders and diseases, identify harmful effects from exposure to mitochondrial toxicants, and better predict which chemicals will target mitochondria.

REFERENCES

1. Bess, A. S., Crocker, T. L., Ryde, I. T., & Meyer, J. N. (2012). Mitochondrial dynamics and autophagy aid in removal of persistent mitochondrial DNA damage in *Caenorhabditis elegans*. *Nucleic acids research*, *40*(16), 7916-7931.
2. The North American Mitochondrial Disease Consortium. (n.d.). *Overview of mitochondrial diseases*. Retrieved from <http://rarediseasesnetwork.epi.usf.edu/namdc/learnmore/index.htm>
3. Meyer, J. N., Leung, M. C., Rooney, J. P., Sandoel, A., Hengartner, M. O., Kisby, G. E., & Bess, A. S. (2013). Mitochondria as a target of environmental toxicants. *toxicological sciences*, *134*(1), 1-17.
4. Li, N., Sioutas, C., Cho, A., Schmitz, D., Misra, C., Sempf, J., ... & Nel, A. (2003). Ultrafine particulate pollutants induce oxidative stress and mitochondrial damage. *Environmental health perspectives*, *111*(4), 455.
5. Meyer, J. N. (2010). QPCR: a tool for analysis of mitochondrial and nuclear DNA damage in ecotoxicology. *Ecotoxicology*, *19*(4), 804-811.
6. Bess, A. S., Ryde, I. T., Hinton, D. E., & Meyer, J. N. (2013). UVC-Induced Mitochondrial Degradation via Autophagy Correlates with mtDNA Damage Removal in Primary Human Fibroblasts. *Journal of biochemical and molecular toxicology*, *27*(1), 28-41.
7. Leung, M. C., Rooney, J. P., Ryde, I. T., Bernal, A. J., Bess, A. S., Crocker, T. L., ... & Meyer, J. N. (2013). Effects of early life exposure to ultraviolet C radiation on mitochondrial DNA content, transcription, ATP production, and oxygen consumption in developing *Caenorhabditis elegans*. *BMC Pharmacology and Toxicology*, *14*(1), 9.
8. Hillier, L. W., Coulson, A., Murray, J. I., Bao, Z., Sulston, J. E., & Waterston, R. H. (2005). Genomics in *C. elegans*: so many genes, such a little worm. *Genome research*, *15*(12), 1651-1660.
9. Okimoto, R., Macfarlane, J. L., Clary, D. O., & Wolstenholme, D. R. (1992). The mitochondrial genomes of two nematodes, *Caenorhabditis elegans* and *Ascaris suum*. *Genetics*, *130*(3), 471-498.
10. Murgatroyd, C., & Spengler, D. (2010). Histone tales: echoes from the past, prospects for the future. *Genome biology*, *11*(2), 105.
11. Thannickal, V. J., & Fanburg, B. L. (2000). Reactive oxygen species in cell signaling. *American Journal of Physiology-Lung Cellular and Molecular Physiology*, *279*(6), L1005-L1028.

12. Di Giulio, Richard T., and Joel N. Meyer. "Reactive oxygen species and oxidative stress." *The toxicology of fishes* (2008): 273-324.
13. Liu, Y., Fiskum, G., & Schubert, D. (2002). Generation of reactive oxygen species by the mitochondrial electron transport chain. *Journal of neurochemistry*, 80(5), 780-787.
14. Lewis, W., Copeland, W. C., & Day, B. J. (2001). Mitochondrial DNA Depletion, Oxidative Stress, and Mutation: Mechanisms Of Dysfunction from Nucleoside Reverse Transcriptase Inhibitors. *Laboratory investigation*, 81(6), 777.
15. Lee, H. C., & Wei, Y. H. (2005). Mitochondrial biogenesis and mitochondrial DNA maintenance of mammalian cells under oxidative stress. *The international journal of biochemistry & cell biology*, 37(4), 822-834.
16. Houtkooper, R. H., Mouchiroud, L., Ryu, D., Moullan, N., Katsyuba, E., Knott, G., ... & Auwerx, J. (2013). Mitonuclear protein imbalance as a conserved longevity mechanism. *Nature*, 497(7450), 451-457.
17. Miwa, S., & Brand, M. D. (2003). Mitochondrial matrix reactive oxygen species production is very sensitive to mild uncoupling. *Biochemical Society Transactions*, 31(6), 1300-1301.
18. Leung, M. C., Williams, P. L., Benedetto, A., Au, C., Helmcke, K. J., Aschner, M., & Meyer, J. N. (2008). *Caenorhabditis elegans*: an emerging model in biomedical and environmental toxicology. *Toxicological Sciences*, 106(1), 5-28.
19. Yang, W., & Hekimi, S. (2010). A mitochondrial superoxide signal triggers increased longevity in *Caenorhabditis elegans*. *PLoS biology*, 8(12), e1000556.
20. Lee, S. J., Hwang, A. B., & Kenyon, C. (2010). Inhibition of Respiration Extends *C. elegans* Life Span via Reactive Oxygen Species that Increase HIF-1 Activity. *Current Biology*, 20(23), 2131-2136.
21. Zhang, X., Rosenstein, B. S., Wang, Y., Lebwohl, M., & Wei, H. (1997). Identification of possible reactive oxygen species involved in ultraviolet radiation-induced oxidative DNA damage. *Free Radical Biology and Medicine*, 23(7), 980-985.
22. Haynes, C. M., & Ron, D. (2010). The mitochondrial UPR—protecting organelle protein homeostasis. *Journal of cell science*, 123(22), 3849-3855.
23. Bratic, I., Hench, J., Henriksson, J., Antebi, A., Bürglin, T. R., & Trifunovic, A. (2009). Mitochondrial DNA level, but not active replicase, is essential for *Caenorhabditis elegans* development. *Nucleic acids research*, 37(6), 1817-1828.

24. Doonan, R., McElwee, J. J., Matthijssens, F., Walker, G. A., Houthoofd, K., Back, P., ... & Gems, D. (2008). Against the oxidative damage theory of aging: superoxide dismutases protect against oxidative stress but have little or no effect on life span in *Caenorhabditis elegans*. *Genes & development*, 22(23), 3236-3241.
25. Gems, D., & Doonan, R. (2009). Antioxidant defense and aging in *C. elegans*. *Cell Cycle*, 8(11), 1681-1687.
26. Back, P., Matthijssens, F., Vlaeminck, C., Braeckman, B. P., & Vanfleteren, J. R. (2010). Effects of sod gene overexpression and deletion mutation on the expression profiles of reporter genes of major detoxification pathways in *Caenorhabditis elegans*. *Experimental gerontology*, 45(7), 603-610.
27. Graziewicz, M. A., Day, B. J., & Copeland, W. C. (2002). The mitochondrial DNA polymerase as a target of oxidative damage. *Nucleic acids research*, 30(13), 2817-2824.
28. Lee, H. C., & Wei, Y. H. (2005). Mitochondrial biogenesis and mitochondrial DNA maintenance of mammalian cells under oxidative stress. *The international journal of biochemistry & cell biology*, 37(4), 822-834.
29. Virbasius, J. V., & Scarpulla, R. C. (1994). Activation of the human mitochondrial transcription factor A gene by nuclear respiratory factors: a potential regulatory link between nuclear and mitochondrial gene expression in organelle biogenesis. *Proceedings of the National Academy of Sciences*, 91(4), 1309-1313.
30. Van Raamsdonk, J. M., & Hekimi, S. (2009). Deletion of the mitochondrial superoxide dismutase sod-2 extends lifespan in *Caenorhabditis elegans*. *PLoS genetics*, 5(2), e1000361.
31. Yoneda, T., Benedetti, C., Urano, F., Clark, S. G., Harding, H. P., & Ron, D. (2004). Compartment-specific perturbation of protein handling activates genes encoding mitochondrial chaperones. *Journal of cell science*, 117(18), 4055-4066.
32. Durieux, J., Wolff, S., & Dillin, A. (2011). The cell-non-autonomous nature of electron transport chain-mediated longevity. *Cell*, 144(1), 79-91.
33. Haynes, C. M., Yang, Y., Blais, S. P., Neubert, T. A., & Ron, D. (2010). The Matrix Peptide Exporter HAF-1 Signals a Mitochondrial UPR by Activating the Transcription Factor ZC376.7 in *C. elegans*. *Molecular cell*, 37(4), 529-54.

34. Shen, X., Ellis, R. E., Lee, K., Liu, C. Y., Yang, K., Solomon, A., ... & Kaufman, R. J. (2001). Complementary Signaling Pathways Regulate the Unfolded Protein Response and Are Required for *C. elegans* Development. *Cell*, *107*(7), 893-903.
35. Zhang, X., Rosenstein, B. S., Wang, Y., Lebwohl, M., & Wei, H. (1997). Identification of possible reactive oxygen species involved in ultraviolet radiation-induced oxidative DNA damage. *Free Radical Biology and Medicine*, *23* (7), 980-985.
36. Yakes, F. M., & Van Houten, B. (1997). Mitochondrial DNA damage is more extensive and persists longer than nuclear DNA damage in human cells following oxidative stress. *Proceedings of the National Academy of Sciences*, *94*(2), 514-519.
37. Cooke, M. S., Evans, M. D., Dizdaroglu, M., & Lunec, J. (2003). Oxidative DNA damage: mechanisms, mutation, and disease. *The FASEB Journal*, *17*(10), 1195-1214.
38. Santos, J. H., Meyer, J. N., Mandavilli, B. S., & Van Houten, B. (2006). Quantitative PCR-based measurement of nuclear and mitochondrial DNA damage and repair in mammalian cells. In *DNA Repair Protocols* (pp. 183-199). Humana Press.
39. Braeckman, B. P., Houthoofd, K., De Vreese, A., & Vanfleteren, J. R. (2002). Assaying metabolic activity in ageing *Caenorhabditis elegans*. *Mechanisms of ageing and development*, *123*(2), 105-119.